

# UNIVERSITÀ DEGLI STUDI DI PADOVA

**Dipartimento di Fisica e Astronomia "Galileo Galilei"**

**Corso di Laurea in Fisica**


**Tesi di Laurea**

# COSMOLOGICAL DYNAMICS OF "UNIFIED DARK MATTER" MODELS BASED ON PERFECT FLUIDS

**(Dinamica cosmologica di modelli di "Unified Dark Matter" basati su fluidi perfetti)**


**Relatore**

**Prof. Sabino Matarrese**

**Correlatore**

**Dr. Daniele Bertacca**

**Laureando**

**Renato Trentin**


**Anno Accademico 2021/2022**

**Abstract**

[ENG] The current evidence of an accelerated expansion of the universe is briefly discussed from an historical perspective and in the context of General Relativity, the concept of dark energy is introduced. The presence of extra mass which doesn't interact electromagnetically, called dark matter, is also shortly adressed. Given the fluid equation describing the evolution of the energy density $\rho$ of the universe for FLRW models, a barotropic non-linear equation of state (EoS) $P(\rho)$ is chosen, specifically the quadratic form $P(\rho) = P_0 + \alpha\rho + \beta\rho^2$, already discussed by Ananda and Bruni in [1]. This particular form serves as a general approximation for every $P(\rho)$, as it is the Taylor expansion up to the second order about $\rho = 0$. The EoS is studied in the high and low energy regimes and ultimately the full EoS is considered. The cosmological behaviours are discussed and compared. In detail, the change in the free parameters is explored in its consequences on closed, open and flat geometrical models of space-time, standard and phantom behaviours are found along with different possibilities for future/past singularities. The whole analysis is done using the theory of dynamical systems.

**Abstract**

[ITA] L'attuale evidenza di un'espansione accelerata dell'universo viene brevemente discussa da una prospettiva storica e nel conteso della Relatività Generale, viene introdotto il concetto di energia oscura. La presenza di massa in eccesso che non interagisce elettromagneticamente, chiamata materia oscura, viene anch'essa brevemente affrontata. A partire dall'equazione del fluido che descrive l'evoluzione della densità di energia $\rho$ dell'universo per i modelli FLRW, un'equazione di stato (EoS) barotropica e non lineare $P(\rho)$ viene scelta, nello specifico nella forma quadratica $P(\rho) = P_0 + \alpha\rho + \beta\rho^2$, già discussa da Ananda e Bruni in [1]. Questa forma serve in generale da approssimazione per qualsiasi $P(\rho)$, questo perchè essa è l'espansione in serie di Taylor troncata al secondo ordine rispetto a $\rho = 0$. La EoS viene studiata nei regimi di alta e bassa energia ed infine si considera la EoS completa. I comportamenti cosmologici che insorgono vengono discussi e comparati. Nel dettaglio, una variazione dei parametri presenti viene esplorata nelle sue conseguenze sui modelli geometrici chiusi, aperti e piatti dello spazio-tempo, vengono trovati comportamenti standard e comportamenti fantasma assieme a diverse possibilità per le singolarità future/passate. L'analisi viene fatta con l'ausilio della teoria dei sistemi dinamici.

# Contents

# Introduction

To create a cosmological model one must first choose a theory of gravity and secondly a way to describe the energy-matter distribution present in the universe, once these are established, detailed predictions on the evolution of space-time can be made. In this section we will present the fundamental results of general relativity (GR), the standard and most experimentally verified gravitational theory, which we will use, whilst the latter will be taken into consideration in the next section. We will also shortly adress the presence of "extra mass" in our universe which doesn't interact electromagnetically (dark matter), along with the evidence of an accelerated expansion for our universe and introduce the notion of dark energy, which is a way to describe the negative pressure that drives this phenomena.

## 0.1 The expansion of the universe

The building blocks of the theory of general relativity (GR) are the 10, non-linear, Einstein field equations:

$$R_{\mu\nu} - \frac{1}{2} g_{\mu\nu} R = \frac{8\pi G}{c^4} T_{\mu\nu} \tag{1}$$

Which connect the sources of the gravitational field, in the form of the stress-energy tensor $T_{\mu\nu}$, to the Ricci tensor $R_{\mu\nu}$ and the Ricci scalar $R$ - both contractions of the Riemann tensor $R^{\sigma}_{\mu\nu\rho}$ - and to the metric tensor $g_{\mu\nu}$[1]. $R^{\sigma}_{\mu\nu\rho}$ and $g_{\mu\nu}$ give us information respectively on the curvature and the metric of the Riemmanian manifold which is space-time. Also, $G$ is the universal gravitational constant[2] and $c$ the speed of light in vacuum[3]. Provided that we choose GR as our theory of gravity, these equations tell us that once the components of the stress-energy tensor are specified, that is, when we specify the matter and energy content of the universe, we possess all the information necessary to predict the evolution of the entirety of space-time.

There is the possibility, however, to introduce another (constant) term in the Einstein field equations, due to the fact that these are not unique. In fact, this is exactly what Einstein did when he first proposed them in 1917, with the equations that read:

$$R_{\mu\nu} - \frac{1}{2} g_{\mu\nu} R + g_{\mu\nu}\Lambda = \frac{8\pi G}{c^4} T_{\mu\nu} \tag{2}$$

$\Lambda$ was baptised *cosmological constant* and was originally chosen by Einstein to be positive, in the attempt to describe a static universe, instead of the expanding/contracting solution predicted in the absence of this extra term. A way of seeing it is that the effect of a positive $\Lambda$ is equivalent to that of an "anti-gravitational" force, in particular preventing the universe from collapsing onto itself. This choice was proved to be a

[1] Cf. [6].
[2] $G = 6.674^{-11} kg^{-1} m^3 s^{-2}$
[3] $c = 299792458 ms^{-1}$

poor one: indeed subsequent works showed that the model was unstable for small perturbations[4], which led once again to an expanding/contracting solution, hence it was believed it could not arise in the first place. The final proof of a non-static universe came in 1929, when Hubble first observed[5] the expansion of the universe formulating the empirical law that takes his name, that is:

$$\vec{v} = H_0 \vec{r} \tag{3}$$

Here $\vec{v}$ is the velocity of recession of the galaxies from us and $\vec{r}$ the distance between us and them, $H_0$ is the present value[6] of the *Hubble parameter*[7] telling us the current expasion rate of the universe. The *cosmological principle*, which states that on the largest scales the universe is spatially homogeneous and isotropic, assures us that we are not privileged (nor underprivileged) observers, hence every galaxy is moving away from one another according to Hubble's law[8]. In the scenario of a uniform expansion a particularly convenient set of coordinates can be chosen: if $\vec{r}$ is the position vector connecting the two celestial objects that we want to consider, the *comoving coordinates* are such that $\vec{r} = a(t)\vec{x}$, where $\vec{x}$ is the *comoving distance* which is constant in time and $a(t)$ is the parameter that takes into account the actual expansion (or contraction) of the physical coordinates, it is called *scale factor*. Noticing that the velocity of recession is the time derivative of $\vec{r}$, and using the fact that $\vec{x}$ is time independent, we arrive to a useful expression of the Hubble parameter: $H = \dot{a}/a$.[9] We can use this to write the most important equation of standard cosmology, the *Friedmann equation*, in the form:

$$H^2 = \frac{8\pi G}{3}\rho - \frac{Kc^2}{a^2} \tag{4}$$

Where $K$ is the curvature of the universe and it can be 0, +1 or −1 respectively for flat, closed and open models. It is more practical to introduce units such that $8\pi G \equiv 1$ and $c \equiv 1$, which we will use from now on, so the equation above becomes:

$$H^2 = \frac{1}{3}\rho - \frac{K}{a^2} \tag{5}$$

The Friedmann equation is the first integral[10] of the autonomous and non-linear system given by the fluid equation (conservation of energy), which we will meet shortly, and the Raychaudhuri equation describing FLRW[11] models in a GR context. Specifically, in the chosen units the Raychaudhuri equation reads:

$$\dot{H} = -H^2 - \frac{1}{6}(\rho + 3P) \tag{6}$$

Now, taking a step back, we had come to the point in which, due to Hubble's empirical proof of an expanding universe, the cosmological constant constant that gave rise to a static universe was no more needed, so much so that it was almost forgotten up until the late 1990s, when a new discovery was made. Via observations of type Ia supernovas, it was seen for that the universe is expanding at an accelerated

[4] See the generalized Einstein universes that are found in throughout the analysis that follows.

[5] Actually, the first evidence of such came from Vesto Slipher in 1912, when he noticed via redshift observations that some spiral galaxies were moving away from us, although he did not grasp the cosmological implications of the discovery.

[6] $H_0 = 100\text{h}\ kms^{-1}Mpc^{-1}$ is a standard parametrization. The value of h is currently debated. In 2021 the *SH0ES* project measured it as $0.73 \pm 0.01$ via standard candles method, while other indirect measures give somewhat lower estimates, such as $0.673 \pm 0.012$ by the analysis of the *Planck* satellite observations. However it is safe to say that h$\approx 0.7$ within a small error of the order of a some percent.

[7] Historically known as the *Hubble constant*.

[8] Not taking into account the random motions that galaxies have in respect to one another, that is, ignoring the *peculiar velocities*. Without neglecting peculiar velocities Hubble's law would become: $\vec{v} = H_0\vec{r} + \vec{v}_{pec}$. The peculiar velocity of the Milky Way is approximately $400kms^{-1}$, which is somewhat typical for a galaxy. Thus we see that what we just stated works really well with very distant galaxies, where the $v_{pec}$ doesn't contribute much, but not for neighbouring galaxies.

[9] In this script, the dot over the variable will always indicate the time derivative.

[10] This is true only once an equation of state $P = P(\rho)$ is specified.

[11] The *Friedmann-Lemaître-Robertson-Walker* metric is the exact solution in GR describing a homogeneous, isotropic, expanding/contracting path-connected universe.

rate [8]. One of the possible explanations is to summon the argument of dark energy, an unknown form of energy that provides the negative pressure needed for the accelerated expansion. In the simplest case, dark energy can be described as the cosmological constant itself and it is generally accepted in standard cosmology to be so, although this description is not devoid of problems, as the theoretical predictions of quantum field theory strongly disagree with the value based on the empirical observations (cf. [9]).

## 0.2 Dark matter

Returning to the Friedmann equation we see that there is a particular energy density, called *critical density*[12] $\rho_C$, for which the geometry of the universe at a certain time is flat, that is $\rho_C = 3H^2$. The common use is to express the total energy density with the dimensionless *density parameter* $\Omega$, defined as $\Omega(t) \equiv \rho/\rho_C$. This is helpful, in that subdividing $\rho$ in its different contributions gives an idea of how the energy is distributed in our universe. For baryonic matter, i.e. the "conventional" matter made up by protons and neutrons (the elements gathered in the periodic table), the current estimate gives $\Omega_B \approx 0.05$[13]. We know that the current energy density of the universe is close to the critical value, at least within 10%, so in total $\Omega$ must be pretty close to 1. The dark energy contribution is estimated to account for approximately 69% of the total energy density, so we are left with approximately 26% of energy of unseen matter, namely:

$$\Omega_{CDM} \approx 0.26 \tag{7}$$

The CDM subscript stands for "cold dark matter". Cold in the sense that at the present time it is non-relativistic, and dark matter in that we don't really know of what it is made up of, if it is one or more species of particles and so on. This is due to the fact that such matter does not interact with electromagnetic fields and our experimental evidence of its presence is indirect. Although we will not adress the evidences of dark matter in this script, we mention that proofs of its presence come from gravitational arguments like the analysis of galaxy rotation curves, gravitational lensing observations, the theory of Big Bang Nucleosynthesis (BBN), the analysis of the cosmic microwave background (CMB) and so on.

## 0.3 The fluid equation and dark energy

Although a rigorous derivation of the fluid equation has to take into account GR, we can derive it by using some simple and general thermodynamical arguments. In fact, conservation of energy can be expressed as the first law of thermodynamics, that is

$$dE + PdV = TdS \tag{8}$$

Here $E$, $V$ and $T$ are, respectively, the internal energy, the volume and the temperature of the system. $P$ is the pressure (force per unit area) exerted by the system on the environment and $S$ is the entropy. If we consider a gas trapped in a box of volume $V$, a reversible[14] adiabatic expansion is one for which there is no exchange of energy in the form of mass or heat, in other words the only variation of energy is given by the work done by the gas particles in order to move the sides of the box. In this case the variation of entropy is zero, and, invoking the time dependence of the first law we arrive to

$$\frac{dE}{dt} = -P\frac{dV}{dt} \tag{9}$$

[12] At the present time, with $H_0$ as Hubble parameter, we have the estimate: $\rho_C = 2.78h^{-1} \times 10^{11} \frac{M_\odot}{(h^{-1}Mpc)^3}$, where $M_\odot \approx 2 \times 10^{30} kg$ is the solar mass and the *megaparsec* is $Mpc = 10^6 pc = 3.261 \times 10^6$ light years $= 3.086 \times 10^{22} m$.

[13] For these and the following estimates see [7] (cf. also [5]).

[14] In a thermodynamical sense this means that every change in the system happens via infinitesimal quasistatic variations of its extensive properties (pressure, temperature, ...), so that the change can be reverted and the initial state reobtained. In this way the process is continuous as at each moment the system passes through states of equilibrium.

Replacing the gas with a fluid of time dependant energy density $\rho(t)$ inside a region of co-moving spherical volume $V_0$ will serve us as model for an expanding (or contracting) universe. The change in time of the volume is

$$V(t) = \frac{4\pi}{3} r^3(t) = \frac{4\pi}{3} a^3(t) x^3 = a^3(t) V_0 \tag{10}$$

This means that

$$\frac{dV(t)}{dt} = 3a^2(t)\dot{a}(t)V_0 \tag{11}$$

On the other hand, we can write the total energy of the fluid in the volume as

$$E(t) = \frac{4\pi}{3} r^3(t)\rho(t) = a^3(t)V_0\rho(t) \tag{12}$$

Hence

$$\frac{dE(t)}{dt} = 3a^2(t)\dot{a}(t)V_0\rho(t) + a^3(t)V_0\dot{\rho}(t) \tag{13}$$

Altogether with the first law of thermodynamics we arrive to the fluid equation

$$\dot{\rho} = -3H(P + \rho) \tag{14}$$

In order to solve this differential equation, an equation of state (EoS) for the pressure is needed. It is generally assumed that a unique pressure is associated with each energy density (barotropic fluid), $P = P(\rho)$. Once this is set, the model for the universe is complete. In standard cosmology it is usually taken into consideration a linear EoS of the form $P = w\rho$, for example for standard baryonic matter (non relativistic, pressurless) $w = 0$, for radiation $w = 1/3$. However, an accelerated expansion for the universe is achieved only for $w < -1/3$[15], for which the fluid behaves as what has been dubbed "*dark energy*". The simplest form of dark energy is indeed the cosmological constant itself, for which $w = -1$. In fact, describing $\Lambda$ as a fluid with the energy density:

$$\rho_\Lambda = \Lambda = const. \tag{15}$$

We can add it up to the energy density $\rho$ of the fluid in the Friedmann equation:

$$H^2 = \frac{1}{3}(\rho + \rho_\Lambda) - \frac{K}{a^2} \tag{16}$$

The fluid equation for $\rho_\Lambda$ gives:

$$\rho_\Lambda = -P_\Lambda \tag{17}$$

Hence $\rho_\Lambda$ provides the negative pressure needed for the accelerated expansion, as desired. It is important to note that we haven't made any implicit assumption on what dark energy actually is, we just described it as a fluid that - in general - causes the negative pressure needed. This said, dark energy is generally associated with the energy density of vacuum, moreover, as we have said, in the framework of the standard cosmological model theoretical predictions for $\Lambda$ give a value that is way larger than the estimates derived by empirical data[16]. This, together with the need to take into account, inside the Friedmann equation, also for a dark matter component, leads to consider alternative possibilities that reproduce the dark energy behaviour without leading to discrepancies with observations. One of the possibilities is to modify the EoS and explore what kind of models arise in different scenarios and this is the road that we will take in the present script.

[15] See the next chapter.

[16] This is known as the "cosmological constant problem".

# The Quadratic Equation of State

In this chapter we will introduce the specific form of the EoS that we will analyze. The different regimes at which we will look will be presented, together with the tools that will be used to understand the dynamics of the solutions. Some first considerations on the essential behavioural traits of the solutions are adressed.

## 0.4 Effective cosmological constant

Let us recall the fluid equation:

$$\dot{\rho} = -3H(\rho + P)$$

We immediately see that if $P = -\rho$ we meet a stationary point for the energy density, this due to the time derivative becoming zero. It is exactly what happens for the cosmological constant fluid, as previously seen. Because of this we will say that, for the general barotropic EoS $P = P(\rho)$, if there exists a $\rho_\Lambda$ such that:

$$P(\rho_\Lambda) = -\rho_\Lambda \tag{18}$$

Such $\rho_\Lambda$ acts as an *effective cosmological constant*, because it plays the same role for the dynamical system of that given by a cosmological constant term. We note that nothing prevents, in general, from the possibility that more than one $\rho_\Lambda$ is present: this will depend on the specific form of $P(\rho)$.

## 0.5 Accelerated phases and asymptotical tendencies

Given that $H \equiv \dot{a}/a$, differentiating the Hubble parameter in respect of the time $t$ yields:

$$\dot{H} = \frac{\ddot{a}}{a} - \frac{\dot{a}}{a^2} \cdot \dot{a} \tag{19}$$

Which means that:

$$\dot{H} + H^2 = \frac{\ddot{a}}{a} \tag{20}$$

Since $\ddot{a}$ is the parameter that regulates the acceleration/deceleration of the expansion or of the contraction of the universe, taking into consideration (6), an accelerated phase is achieved for[17]:

$$P(\rho) < -\frac{\rho}{3} \tag{21}$$

In addition to this, we can rewrite (14) in a convenient form to characterize another kind of behaviour. Defining $\tau \equiv \ln a$ we have that $d\tau = da/a$, which leads to:

$$\frac{d\rho}{dt}\frac{1}{H} = \frac{d\rho}{d\tau} \tag{22}$$

[17]This limited only to the case in which we use General Relativity as our theory of gravity. Generally speaking, other theories may produce different conditions for such behaviour.

Here we assume $H > 0$. Using (14) we arrive to:

$$\frac{d\rho}{d\tau} = -3[\rho + P(\rho)] \tag{23}$$

We find that if $\rho + P(\rho) < 0$ we meet a region in which the fluid behaves counterintuitevely. In fact, in this region an expansion of the universe provides an increase in the energy density, whilst on the other side a contratcion leads to a decrease of the latter (see [12, 13]). A cosmological fluid that follows this dynamic has been called *phantom fluid* [11]. We see that, if there are fixed points (one or more) for (23), they are $\rho_\Lambda$. These points behave as attractors[18] for (23) if $\rho + P(\rho) < 0$ (phantom fluid) for $\rho < \rho_\Lambda$ and $\rho + P(\rho) > 0$ (standard fluid) for $\rho > \rho_\Lambda$, meaning that the orbits which asympotically approach $\rho_\Lambda$ do so in the future. Vice versa, if the opposites of all the conditions we just mentioned are met, the point is a repeller (i.e. an attractor in the past). If $\rho_\Lambda$ satisfies $\rho + P(\rho) < 0$ or $\rho + P(\rho) > 0$ for both $\rho < \rho_\Lambda$ and $\rho > \rho_\Lambda$, the point is a shunt[19].

## 0.6 The EoS and its regimes

In our analysis, following the trail set by Ananda and Bruni in [1], we will take into consideration a non-linear equation of state for the cosmological fluid and do a Taylor expansion about $\rho = 0$, which gives:

$$P(\rho) = P\Big|_{\rho=0} + \rho \cdot \frac{dP}{d\rho}\Big|_{\rho=0} + \frac{\rho^2}{2} \cdot \frac{d^2P}{d\rho^2}\Big|_{\rho=0} + \mathcal{O}(\rho^3) \tag{24}$$

It can be proved [10] that - by a regrouping of terms - the Taylor expansion truncated at the second order and done about the present day energy density $\rho_0$ can be written in the general form:

$$P(\rho) = P_0 + \alpha\rho + \beta\rho^2 \tag{25}$$

The three free parameters $P_0$, $\alpha$ and $\beta$ reproduce, by varying, many different cosmological scenarios, which will be the focus of our study. It is important to stress that this is an approximation valid for every non-linear barotropic EoS, hence the generality, and it includes the exact one only if the quadratic EoS in "the correct one" for a specific set of parameters. From this standpoint we will investigate which of these dark energy models could possibly be closer to the reality as we know it, furthermore it is possible that these kind of EoS allow also for the description of dark matter, providing a framework for the so called Unified Dark Matter (UDM) models. The latter try to unify the two concepts under a single entity, which could explain a possible influence exerted by dark energy in the process of clustering undergone by dark matter [2]. Albeit stricly relevant, the topic of UDM won't be adressed in the present script, we will focus instead solely on the dark energy component.

In order to gain a more detailed understanding of the behaviours that may arise from the chosen EoS, the analysis will be at first subdivided in two different regimes: the high energy regime will be the limit case in which the energy density term is predominant, we will study the equation:

$$P_{HE}(\rho_{HE}) = \alpha\rho_{HE} + \beta\rho_{HE}^2 \tag{26}$$

And the low energy regime will be the limit in which the quadratic term becomes neglectable, the equation this time will be:

$$P_{LE}(\rho_{LE}) = P_0 + \alpha\rho_{LE} \tag{27}$$

The subscripts $HE$ and $LE$ refer to the ranges of energy density and they serve as a reminder that the two equations presented are limit cases of the full EoS, which will be presented in our last analysis.

[18] See the section "Characterization of fixed points in a dynamical system" for detailed prescriptions on the nature of equilibriums in the theory of dynamical systems.

[19] A shunt is an attractor for one of the orbits that asymptotically approaches it and a repeller for the other one.

## 0.7 Singularities

With our choice of the EoS, the singularities that may arise are much richer than the standard "Big Bang/Big Crunch" asymptotical behaviours, for example we will encounter cases in which the energy density or the scale factor diverge, or possibly both (in a phantom region). In detail, we will say that a certain singularity is a *Big Bang* if $a \to 0$ and $\rho \to \infty$ in the past, *Big Crunch* if the same condition happens in the future. Furthermore - provided that $t_\star$, $a_\star$ ($\neq 0$), $\rho_\star$ and $|P_\star|$ are constant values respectevely of $t$, $a$, $\rho$ and $|P|$ to be determined - as done in [1] (cf. also [14], [16]) we will classify the other possible singularities in the following manner:

1. *Type I* ( or *Big Rip*) if, for $t \to t_\star$, we have that $a \to \infty$, $\rho \to \infty$ and $|P| \to \infty$.
2. *Type II* (or *Sudden*) if, for $t \to t_\star$, we have that $a \to a_\star$, $\rho \to \rho_\star$ or 0 and $|P| \to \infty$.
3. *Type III* if, for $t \to t_\star$, we have that $a \to a_\star$, $\rho \to \infty$ and $|P| \to \infty$.
4. *Type IV* if for $t \to t_\star$ we have $a \to a_\star$, $\rho \to \rho_\star$ or 0, $|P| \to |P_\star|$ or 0 and the derivatives of $H$ diverge.

## 0.8 Characterization of fixed points in a dynamical system

Let us consider the following planar system of differential equations involving the first time derivatives of the energy density and of the Hubble parameter:

$$\begin{cases} \dot{\rho} = X_1(\rho, H) \\ \dot{H} = X_2(\rho, H) \end{cases} \tag{28}$$

If we define the vector $z = z(t) \equiv (\rho(t), H(t))$, (28) can be expressed in terms of the vector field $X = (X_1(z), X_2(z))$ as:

$$\dot{z} = X(z) = \begin{bmatrix} \dot{\rho} \\ \dot{H} \end{bmatrix} \tag{29}$$

The fixed points of the system are - if they exist - those $z = \bar{z}_i$ who satisfy $X(\bar{z}_i) = 0$, namely the stationary points of the vector field. The information on the dynamical nature[20] of these points can be gained by carrying out a spectral analysis of the linearization of $X(z)$ about $\bar{z}_i$, which gives us an insight on how the solutions behave in the tangent space of $X(\bar{z}_i)$, so the validity is local. All this is done by finding the eigenvalues $\lambda_i$ of the system's Jacobian matrix, $J_X(z) = (\partial X_i/\partial z_j)_{i,j=1,2}$, and evaluating them in each one of the fixed points. In detail, a sufficient condition for instability would be that at least one of the two eigenvalues has positive real part ($\mathfrak{Re}\{\lambda_i\} > 0$ for some $i$); on the other hand a necessary condition for stability would be that all eigenvalues have negative real part ($\mathfrak{Re}\{\lambda_i\} < 0$ for all $i$). Moreover, for an autonomous planar system like this one there is a specific categorization: if the eigenvalues have nonzero real part the fixed point is said to be hyperbolic, specifically: an attractor[21] if both eigenvalues have negative real part and a repeller[22] if both have positive real part, else it is a saddle[23]. If eigenvalues are purely imaginary the fixed point is said to be a center[24].

[20] Cf. [3].

[21] Small perturbations (meaning a local validity) will bring back the system to this (stable) equilibrium. The phase portraits in the neighbourhood of such points are inward nodes or inward spirals.

[22] Solutions tend to "run away" from these points, hence the equilibrium is an unstable one: in fact small perturbations won't allow for the system to return in place. Here we locally have outward nodes or outward spirals.

[23] In this case the behaviour is hybrid, depending on which direction the perturbation is carried out, but there is no general stability.

[24] Phase portraits are locally ellipses.

# High Energy Regime

As we previously mentioned, for high enough energy densities the quadratic term becomes the dominant one in the EoS and in comparison the constant pressure $P_0$ becomes irrelevant. In the present chapter we will analyze the specific case in which, for $\alpha, \beta \neq 0$, we have:

$$P_{HE} = \alpha\rho_{HE} + \beta\rho_{HE}^2 \tag{30}$$

Inserting this equation in (14) and integrating from an arbirtary time $t_0$ to $t$ yields:

$$\dot{\rho}_{HE} = -3\frac{\dot{a}}{a}[\rho_{HE}(\alpha+1) + \beta\rho_{HE}^2]$$

$$\int_{t_0}^{t} \frac{1}{[\rho_{HE}(\alpha+1)+\beta\rho_{HE}^2]}\frac{\partial\rho_{HE}}{\partial t'}dt' \overset{\alpha\neq-1}{=} -\frac{1}{\alpha+1}\int_{t_0}^{t}\left\{-\frac{(\alpha+1)}{\rho_{HE}^2}\frac{1}{[\frac{1}{\rho_{HE}}(\alpha+1)+\beta]}\right\}\frac{\partial\rho_{HE}}{\partial t'}dt' = -3\int_{t_0}^{t}\frac{1}{a}\frac{\partial a}{\partial t'}dt'$$

$$\frac{1}{\alpha+1}\ln\left|\frac{\alpha+1+\beta\rho_{HE}}{\rho_{HE}}\frac{\rho_0}{\alpha+1+\beta\rho_0}\right| = 3\ln\frac{a}{a_0}$$

$$\rho_{HE}(a) = \frac{\rho_0(\alpha+1)}{(\alpha+1+\beta\rho_0)\left(\frac{a}{a_0}\right)^{3(\alpha+1)} - \beta\rho_0} \quad \text{if} \quad \alpha \neq -1$$

Whilst otherwise we have:

$$\int_{t_0}^{t}\frac{1}{\beta\rho_{HE}^2}\frac{\partial\rho_{HE}}{\partial t'}dt' = -\frac{1}{\beta}\left(\frac{1}{\rho_{HE}} - \frac{1}{\rho_0}\right) = -3\ln\frac{a}{a_0}$$

$$\rho_{HE}(a) = \left(\frac{1}{\rho_0} + 3\beta\ln\frac{a}{a_0}\right)^{-1} \quad \text{if} \quad \alpha = -1$$

Where $\rho_0 = \rho_{HE}(t_0)$, $a_0 = a(t_0)$. For this script we will consider only the case in which $\alpha \neq -1$, in order to focus on the broader spectrum of possible values for this parameter, which have not been largely investigated yet[25].

If we want to obtain an effective cosmological constant we need to impose the constraint $P_{HE}(\rho_\Lambda) = -\rho_\Lambda$ and see if some $\rho_\Lambda$ satisfies it, if we do so we obtain:

$$\rho_\Lambda(\alpha+1+\beta\rho_\Lambda) = 0 \tag{31}$$

Excluding the trivial case[26] in which $\rho_\Lambda = 0$, we can define:

$$\rho_\Lambda \equiv -\frac{1}{\beta}(\alpha+1) \tag{32}$$

[25] This equation of state with the choice of $\alpha = -1$ has already been investigated as a dark energy model in [14, 15].

[26] That is of no relevance for our problem since we are looking at "high" energy densities, meaning high enough to be dominant in comparison to $P_0$. Surely high enough to be greater than zero, supposing for the general case $0 \neq P_0 \ll \rho_{HE}$, whatever the order of $P_0$ may be.

Regarding as physical only non-negative values of the energy density and not considering $\rho_\Lambda = 0$ implies that $\rho_\Lambda$ is an effective cosmological constant only if:

$$\frac{1}{\beta}(\alpha+1) < 0 \tag{33}$$

That is: $\alpha < -1$ and $\beta > 0$ or vice versa.

Now, let us recall the functional form of the energy density that we will study:

$$\rho_{HE}(a) = \frac{\rho_0(\alpha+1)}{(\alpha+1+\beta\rho_0)\left(\frac{a}{a_0}\right)^{3(\alpha+1)} - \beta\rho_0} \tag{34}$$

Before proceeding by splitting the analysis in the various subcases (based on the range of the parameters), we will show a specific case of how the analytical results that follow are obtained. For example, let us consider a negative nominator for (34): the denominator must be negative as well, or else we would have an overall negative energy density, so:

$$(\alpha+1+\beta\rho_0)\left(\frac{a}{a_0}\right)^{3(\alpha+1)} < \beta\rho_0 \tag{35}$$

This gives rise to an ulterior categorization. To begin with, if $\alpha+1+\beta\rho_0 > 0$ we have that:

$$\begin{aligned} \rho_0 > -\frac{\alpha+1}{\beta} \quad &\Longrightarrow \left(\frac{a}{a_0}\right)^{3(\alpha+1)} < \left(1+\frac{\alpha+1}{\beta\rho_0}\right)^{-1} \\ &a < a_0 \underbrace{\left(1+\frac{\alpha+1}{\beta\rho_0}\right)^{-\frac{1}{3(\alpha+1)}}}_{\star} \equiv a_\star \end{aligned} \tag{36}$$

An additional condition arises that has to be satisfied: in order to exist for all $\alpha < -1$ the term $(\star)$ must be positive. This leads to the further restriction $-1-\beta\rho_0 < \alpha < -1$. The only other possibility is that $\alpha+1 = -n$ for $n \in \mathbb{N}/\{0\}$ which gives an odd $3n$-root, allowing for a negative radicand. In this subcase the scale factor $a = a(t)$ satisfies $a < a_\star$, hence the expansion cannot continue to infinity, but a Type III singularity is admitted in the future. We can infer this by evaluating the following relevant limit:

$$\rho_{HE}(a) = \frac{(\alpha+1)}{\beta\left[\left(\frac{a}{a_\star}\right)^{3(\alpha+1)} - 1\right]} \overset{a\longrightarrow a_\star^-}{\longrightarrow} \infty \tag{37}$$

On the other hand, if $\alpha+1+\beta\rho_0 < 0$:

$$\rho_0 < -\frac{\alpha+1}{\beta} \quad \Longrightarrow\ a > a_\star \tag{38}$$

Here the Type III singularity is admitted in the past.

To divide the study in cases with different behaviours, we begin by looking at when $\rho_\Lambda$ doesn't define an effective cosmological constant. We will then look at when it does define one and see wether the fluid belongs to a standard or phantom portion of the phase space, this will be determined by the range of the energy density, as $\rho_\Lambda$ (that is now a physical energy density) acts as a separatrix between such regions. The informations on the dynamics of the solutions - for the different curvature terms ($K = 0, \pm 1$) - are gained via the stability analysis presented in the following sections of this chapter. The three cases we have to look at are:

1. *A*: $\rho_\Lambda < 0$

   Using the definition of $a_\star$ that we found in (36), the constraint we have suggests that we can write:

   $$\rho_{HE}(a) = \frac{|\alpha+1|}{|\beta|\left[\left(\frac{a}{a_\star}\right)^{3(\alpha+1)} - 1\right]} \tag{39}$$

   However, there are two possibilities that yield $\rho_\Lambda < 0$, namely:

   - *A1*: $\alpha > -1$ and $\beta > 0$. Imposing a positive energy density implies that $a_\star < a < \infty$, and since:

     $$\lim_{a\to a_\star} \rho_{HE} = \infty, \qquad \lim_{a\to\infty} \rho_{HE} = 0 \tag{40}$$

     The energy density here falls in the range $0 < \rho_{HE} < \infty$. Closed models can have a bounce behaviour, reaching a minumum value of the scale factor ($a_\star$) and after that re-expand, or evolve with a standard bounce at a minimum energy density and scale factor from/to a Type III singularity. Open and flat models display solutions that, once again, can have a past/future Type III singularity and they are correspondigly asymptotical to the fixed point A1 (Minkowski universe), this can happen also for a specific subset of closed models.

   - *A2*: $\alpha < -1$ and $\beta < 0$. Here we have $0 < a < a_\star$ and the relevant limits for $\rho_{HE}$ in this range of the scale factor give the exact opposite results of (40), so in the end we find once again $0 < \rho_{HE} < \infty$. What we see through the limits, since (39) is monotone, immediately tells us that in this case the fluid has phantom behaviour, as the energy density increases when the scale factor does so, and vice versa. A future singularity for $a = a_\star$ is present, for the closed models this singularity is met also in the past and the motion of such solutions is that of a phantom bounce: a contraction takes place, the minimum for both $a$ and $\rho_{HE}$ are reached, then the universe re-expands.

2. *B*: $\rho_\Lambda > 0$ and $\rho_{HE} > \rho_\Lambda$

   We can write:

   $$\rho_{HE}(a) = \frac{\rho_\Lambda}{1 - \left(\frac{a}{a_\star}\right)^{3(\alpha+1)}} \tag{41}$$

   Again, due to the form of $\rho_\Lambda$ we meet two subcases:

   - *B1*: $\alpha < -1$ and $\beta > 0$. For the scale factor we find: $a_\star < a < \infty$. This means that:

     $$\lim_{a\to a_\star} \rho_{HE} = \infty, \qquad \lim_{a\to\infty} \rho_{HE} = \rho_\Lambda \tag{42}$$

     So $\rho_\Lambda < \rho_{HE} < \infty$. The behaviour of the fluid is standard. In general, flat and closed models have a past/future singularity for $a = a_\star$. Closed models display substantial difference depending on which regions the initial conditions fall. Some of them have a singularity in the past/future as the open and flat models do, others contract reaching a minimum scale factor and then re-expand until the finite energy density present at the beginning is met again.

   - *B2*: $\alpha > -1$ and $\beta < 0$. Here $0 < a < a_\star$ and consequently $\rho_\Lambda < \rho_{HE} < \infty$, although this time we are in presence of a phantom fluid. The solutions all have past/future singularities, open and flat models are asymptotical in the future/past to $\rho_\Lambda$, whilst closed models undergo a phantom bounce at minimum scale factor and energy density.

3. *C*: $\rho_\Lambda > 0$ and $\rho_{HE} > \rho_\Lambda$

   For this case we have:
   $$\rho_{HE}(a) = \frac{\rho_\Lambda}{1 + \left(\frac{a}{a_\star}\right)^{3(\alpha+1)}} \tag{43}$$

   With the two subcases that arise:

   - *C1*: $\alpha < -1$ and $\beta > 0$. Here we have $0 < a < \infty$, which means that $0 < \rho_{HE} < \rho_\Lambda$ with a phantom behaviour for the solutions. No singularities are met, the solutions approach in the past/future the finite energy density $\rho_\Lambda$. Flat models in this subset are, in the future/past, asymptotical to a Minkowski universe. Closed models undergo a phantom bounce before re-approaching $\rho_\Lambda$.
   - *C2*: $\alpha > -1$ and $\beta < 0$. Again, $0 < a < \infty$ and $0 < \rho_{HE} < \rho_\Lambda$, this time with a standard behaviour. Apart from that, here the main difference from *C1* is that closed solutions have another type of behaviour: they can either - depending on the subset - contract to a minimum $a$ and $\rho_{HE}$ to then re-expand into a static universe devoid of matter, or oscillate infinitely between two values of the energy density and of the scale factor.

## 0.9 Preliminary stability analysis: high energy regime

If we insert (30) in the autonomous system given by the fluid equation and the Raychaudhuri equation we obtain:
$$\begin{cases} \dot{\rho}_{HE} = -3H\rho_{HE}(\alpha + 1 + \beta\rho_{HE}) \\ \dot{H} = -H^2 - \dfrac{1}{6}\rho_{HE}(1 + 3\alpha + 3\beta\rho_{HE}) \end{cases} \tag{44}$$
The fixed points (constant orbits) are found simply by looking at the zeros of the vector field associated to the system, namely $\dot{\rho}_{HE} = \dot{H} = 0$. With $\dot{\rho}_{HE} = 0$ we find $H = 0$ or $\rho_{HE} = 0$ or $\rho_{HE} = -(\alpha+1)/\beta$, together with the second equation for $\dot{H} = 0$ we arrive to what follows:

| Name | $\rho_{HE}$ | $H$ | Existence |
|---|---|---|---|
| A1 | $0$ | $0$ | $\forall\alpha, \beta$ |
| A2 | $-\frac{1+3\alpha}{3\beta}$ | $0$ | $\frac{\alpha}{\beta} < -\frac{1}{3\beta}$ |
| A3 | $-\frac{\alpha+1}{\beta}$ | $+\sqrt{-\frac{\alpha+1}{3\beta}}$ | $\frac{\alpha}{\beta} < -\frac{1}{\beta}$ |
| A4 | $-\frac{\alpha+1}{\beta}$ | $-\sqrt{-\frac{\alpha+1}{3\beta}}$ | $\frac{\alpha}{\beta} < -\frac{1}{\beta}$ |

Existence conditions for the fixed points have been set imposing a positive energy density, which also grants the existence of the square root in $\mathbb{R}$ appearing in A3 and A4. We will see if these conditions are met later in the analysis. It is interesting to note that A1 corresponds to a Minkowski space-time, for it is a static solution for the Einstein field equations in vacuum, i.e. a non-expanding/contracting universe devoid of matter. It will be interesting to analyze the stability of A1 and see if small perturbations around it can lead to very different types of solutions. A2 is instead a generalization of what goes by the name of "Einstein universe": a static solution with a non-zero density of matter. Here to, it will be crucial to look at the stability of this point to understand if, in the different cases, it is a possibility for the past/future evolution of the present universe. To conclude, A3 and A4 are generalized[27] de Sitter/anti-de Sitter[28] universes, which are spatially flat models: as we will see, they lie on symmetrically

[27] Originally a de Sitter universe contains no ordinary matter.

[28] de Sitter has a positive, in this case effective, cosmological constant, leading to an expansion. Anti-de Sitter has a negative one, for the universe in this case contracts.

opposite points on the parabola given by the Friedmann equation in the case in which $K = 0$ (flat geometry).

The Jacobian matrix of (44) reads:

$$J_X^{HE}(\rho_{HE}, H) = \begin{bmatrix} -3H(\alpha + 1 + 2\beta\rho_{HE}) & -3\rho_{HE}(\alpha + 1 + \beta\rho_{HE}) \\ -\frac{1}{6}(1 + 3\alpha + 6\beta\rho_{HE}) & -2H \end{bmatrix} \tag{45}$$

Evaluating $J_X$ in each one of the fixed points and subsequently calculating the eigenvalues $\lambda_1$, $\lambda_2$ for these matrices gives the following results:

| Fixed point | $\lambda_1(A_i)$ | $\lambda_2(A_i)$ |
|---|---|---|
| A1 | 0 | 0 |
| A2 | $\frac{1+3\alpha}{3}\sqrt{\frac{1}{\beta}}$ | $-\frac{1+3\alpha}{3}\sqrt{\frac{1}{\beta}}$ |
| A3 | $-\frac{2}{3}\sqrt{-\frac{3(\alpha+1)}{\beta}}$ | $(\alpha+1)\sqrt{-\frac{3}{\beta}(\alpha+1)}$ |
| A4 | $\frac{2}{3}\sqrt{-\frac{3(\alpha+1)}{\beta}}$ | $-(\alpha+1)\sqrt{-\frac{3}{\beta}(\alpha+1)}$ |

The classification of the eigenvalues according to the criteria explained in the former chapter will be now done case by case. We will start by considering the sign of $\beta$, and name $HE1$ the case in which $\beta > 0$, $HE2$ the one in which $\beta < 0$. We will then consider the different subcases generated by varying the range of $\alpha$.

## 0.10 $HE1$: $\beta > 0$

In this scenario the eigenvalues for A2 are real and opposite so, as long as $\alpha \neq -1/3$, the point is a saddle. A3 and A4 are respectively an attractor and a repeller when they are real. To sum it up:

| Fixed point | Stability |
|---|---|
| A1 | Undefined |
| A2 | Saddle if $\alpha < -\frac{1}{3}$ and $\nexists$ otherwise |
| A3 | Attractor if $\alpha < -1$ and $\nexists$ otherwise |
| A4 | Repeller if $\alpha < -1$ and $\nexists$ otherwise |

We will now split the case, according to the existence conditions of the fixed points, in three subcases. For all the phase portraits in the script we will choose the following conventions: the fixed points will be marked by red dots; the stable/unstable orbits which subdivide the phase space in regions with different behaviours will be marked in green; each region of the phase space will have a typical behaviour and the orbits in blue will depict particular solutions that describe this broader behaviour; the fixed points lie on the intersections of the nullclines, which correspond to the dashed lines; the arrows in light grey will describe the motion of the solutions in different points of the phase space; lastly, for reference, the equation used to obtain the phase portrait will be shown on the top left, in light blue. For physical reasons the region in which the energy density is negative will not be shown, while for $H$ we consider all values and we note that contracting models have $H < 0$, static ones have $H = 0$ and expanding models $H > 0$.

- *HE1.1*: $\alpha < -1$. Selecting, for example, $\alpha = -\frac{3}{2}$ and $\beta = 1$, for which the conditions studied in this section are met, the underlying phase portrait is obtained:

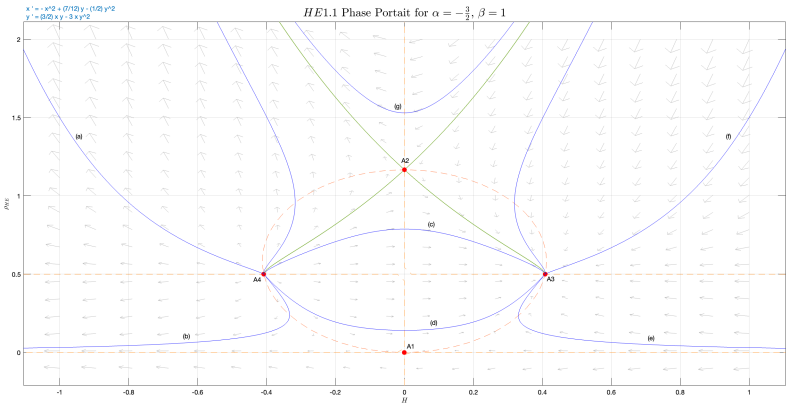


Imposing $K = 0$ in the Friedmann equation gives a spatially flat cosmological model, the parabola $H^2 = \rho_{HE}/3$ acts as separatrix for open models ($K = -1$), whose trajectories lie underneath it, and closed models ($K = 1$) whose trajectories lie above it. In detail: (a), (b), (e) and (f) are closed, every other one represented is open. The horizontal nullcline (*phantom separatrix*) intersecting A3 and A4 separates two regions with very different dynamics: underneath it lies the phantom region (corresponding to the subcase *C1)*, for the fluid behaves increasing in energy density as the universe expands for $H > 0$ and vice versa for $H < 0$. Over this nullcline is the area where the fluid behaves in a standard manner (subcase $B1$), increasing if the universe shrinks in size and decreasing if it expands. The orbits (a) and the unlabelled one to its right represent solutions that move away from the anti-de Sitter universe present in A4, asymptotically approaching an always faster contracting universe with energy density that tends to infinity, the only difference here is that (a) is relative to an open universe whilst the other orbit is for a closed one. (b) moves away from A4 and evolves to a contracting universe with null energy density, and represents an open model. Simmetrically, on the other side (e) evolves from a universe that has an infinite Hubble parameter to a universe that is still expanding but at a finite rate, which reaches a finite energy density (A3) of a flat de Sitter universe in the future, the model is open. The (d) orbit escapes an anti-de Sitter universe, it contracts while the energy density falls, it gradually approaches a stationary point after which the expansion starts and the energy density rises, to end in A3 (de Sitter) in the future, this is also an open model. (c) is similar in some aspects, since it escapes A4 and reaches A3 in the future, but the fluid behaves in a standard manner and the orbit represents a closed model. The regions to which (c) and (d) belong undergo what is dubbed, respectively "*non-phantom/phantom bounce*", for the motion which is undergone. The orbit (f) and the one to its left are respectively for open and closed models, other than this they both evolve by moving away from a past Type I singularity into an expanding flat universe in the future, the energy density decreases approaching the value of A3. At last, (g) is the kind of solution that evolves from a past Type I singularity with an infinitely positive Hubble parameter and energy density, to the same kind of singularity but with an infinitely negative $H$ and $\rho_{HE}$, the model is closed. As mentioned A1, A3 and A4 are stationary orbits describing a flat universe. The upper two green lines are orbits that approach (right) and escape (left) A2, which is a closed stationary solution. The two green lines below A2 are evolving from A2 to A3 (right) and from A4 to A2 (left), they are closed models. The linear stability methods left A1 undefined, but it can be seen that, locally, the orbits above $H^2 = \rho_{HE}/3$ flow from left to right, as does the parabola itself (starting in A4 and ending in A3), whilst under it the flow lines come in from the right and out from the left, but never touching A1 and instead diverging towards A3 and A4 respectively, as (e) and (b) do.

- $HE1.2$: $-1 < \alpha < -\frac{1}{3}$. For the following phase portrait we have set $\alpha = -2/3$ and $\beta = 1$:

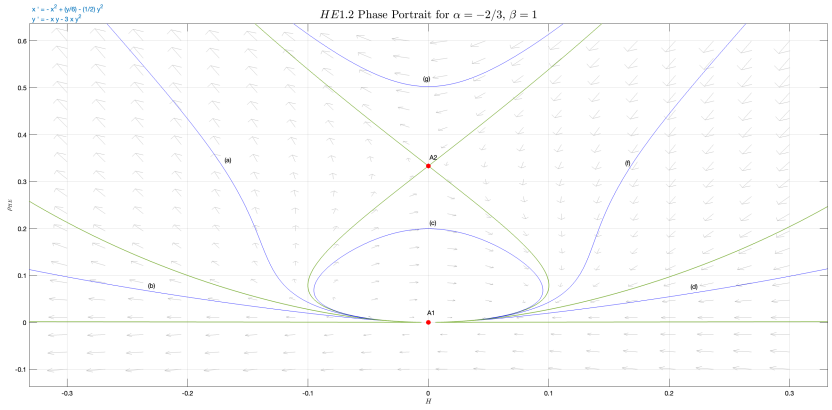


We see that, for this specific subcase, the fluid exhibits a standard behaviour in all of the phase space ($A1$), the phantom separatrix is absent. The parabola in green corresponds to the flat models, above it lie the closed ones, below it the open ones. The (a) orbit evolves leaving a Minkowski universe (the fixed point A1) towards a Type III singularity, on the other hand (f) does the symmetrical opposite under time reversal, they are both closed models. (b) and (d) behave respectively as (a) and (f), but they are open models. (c) evolves by moving away from the Minkowski universe in A1, entering a contracting phase in which a minumum value of the scale factor is reached, the trend then reverts and an expansion takes place until A1 is reached again in the future (standard bounce model). The (g)-type orbits are turn-around models: the universe leaves a Type III singularity, reaches a maximum scale factor, then contracts again into a Type III singularity. The orbits that lie on $\rho_{HE} = 0$ leave ($H < 0$) or approach ($H > 0$) the Minkowski universe present in A1. The green orbits that connect A1 to A2 (Einstein static universe) in $H < 0$ move from A1 to A2 while contracting, the ones in $H > 0$ move from A2 to A1 whilst expanding. The green orbits above the Einstein static universe leave ($H < 0$) or approach ($H > 0$) A2 with a Type III singularity on the other side of the evolution.

- $HE1.3$: $\alpha \geq -\frac{1}{3}$. To obtain the phase portrait below we have set $\alpha = 1$ and $\beta = 1$:

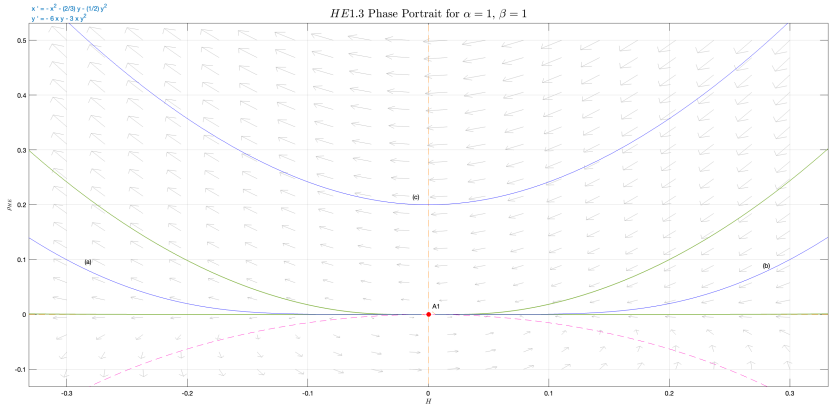


Again, as we found for the previous subcase, all solutions behave in a standard manner, as the energy density increases for a contracting universe, it decreases for an expanding one. The only fixed point that still exists in the $\rho_{HE} > 0$ region, under these conditions, is the Minkowski universe (static, zero energy density) in A1. The (a)-type and (b)-type orbits correspond to open models which respectively leave/approach A1 to/from a Type III singularity. From the green parabola - on which models with zero curvature lie - above, all solutions start and end in a Type III singularity, as the (c) solution (an example of a closed orbit in this region) does.

## 0.11 $HE2$: $\beta < 0$

In this case A2 presents, when it exists, purely imaginary eigenvalues, which makes it a center. On the contrary when A3 and A4 exist they assume saddle nature, A1 remains undefined. Summing up we have:

| Fixed point | Stability |
|---|---|
| A1 | Undefined |
| A2 | Center for $\alpha > -\frac{1}{3}$ and $\nexists$ otherwise |
| A3 | Saddle for $\alpha > -1$ and $\nexists$ otherwise |
| A4 | Saddle for $\alpha > -1$ and $\nexists$ otherwise |

- $HE2.1$: $\alpha < -1$. Here we have set $\alpha = -3/2$ and $\beta = -1$:

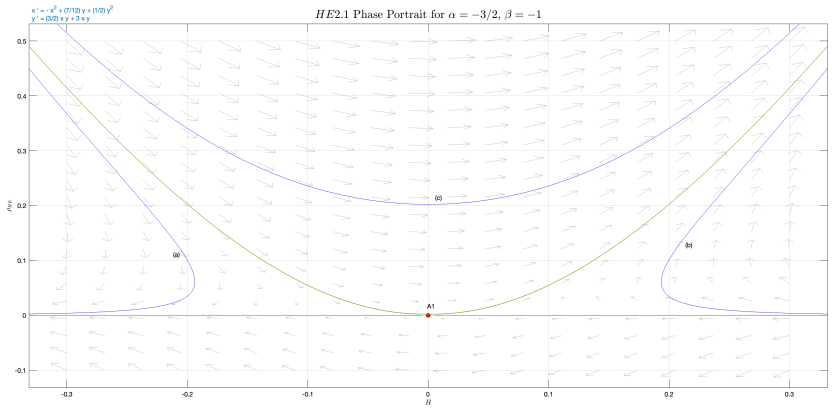


Only A1 exists as fixed point in this subcase. The phase space for $\rho_{HE} > 0$ (physical region) all behaves in phantom manner (condition *A2*). (a) and (b) are open models and they evolve leaving/approaching a Type III singularity in the past/future, (a) contracts asymptotically towards a universe with null energy density and (b) expands its way leaving such universe. Closed models, such as (c), start and end in a Type III singularity, with a turn-around fashion: a minimum $a$ is reached before an the trend inverts. The parabola in green represents the flat models - it is also the separatrix between open and closed models, as in all the other cases - in $H < 0$ solutions leave a Type III singularity to approach a Minkowski universe (A1), in $H > 0$ the solutions have the opposite behaviour.

- $HE2.2$: $-1 < \alpha < -\frac{1}{3}$. Choosing $\alpha = -1/2$ and $\beta = -1$ gives the following phase portrait:

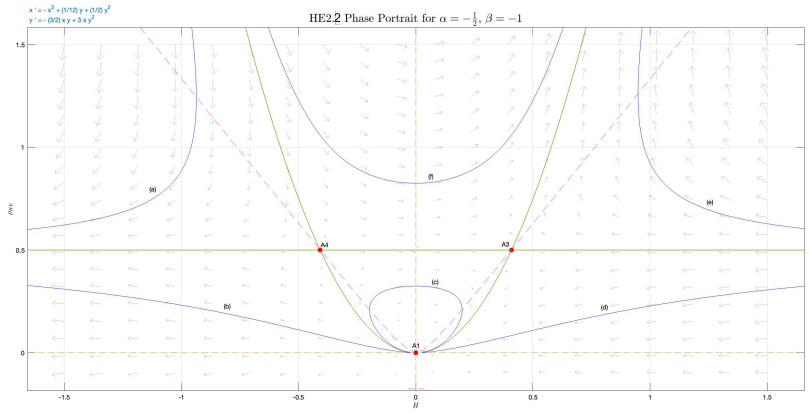


Here the Einstein universe, corresponding to the fixed point A2, is absent. The phase space is

separated, by the green horizontal line ($\rho_{HE} = \rho_\Lambda$) on which A2 and A3 lie, in two regions: above it the solution portray phantom behaviour (*B2*), below it a standard one (*C2*). In detail, the orbits (b), (c) and (d) behave in a standard manner, whilst (a), (e) and (f) are phantom models. The parabola that connects the orbits for flat space-time models with $K = 0$ is shown, the fixed points A4, A1 and A3 lie on it. As for all the other cases, closed models lie over it, open ones under it. Starting from (a), this open phantom model evolves leaving a Type III singularity and approaching the phantom separatrix whilst contracting more and more. (b) escapes from the fixed point A1 (Minkowski), the energy density increases as the universe contracts, eventually reaching the phantom separatrix as well, the model is open. (c) is closed and exhibits a bounce behaviour, it leaves A1 while contracting, reaching a finite value of the scale factor (the contraction then arrests) and energy density - at the intersection with the vertical nullcline - then the trend reverses: an expansion takes place while the energy density decreases, eventually reaching the static and flat universe A1 in the future. The (d) and (e) orbits are the symmetrical opposites (inverting future and past) of, respectively, (b) and (a). The region where (f) lies reunites orbits that start and end in a Type III singularity (turnaround models), passing through a phantom bounce phase.

- $HE2.3$: $\alpha \geq -\frac{1}{3}$. In the phase portrait that follows we have selected $\alpha = 1$ and $\beta = -1$:

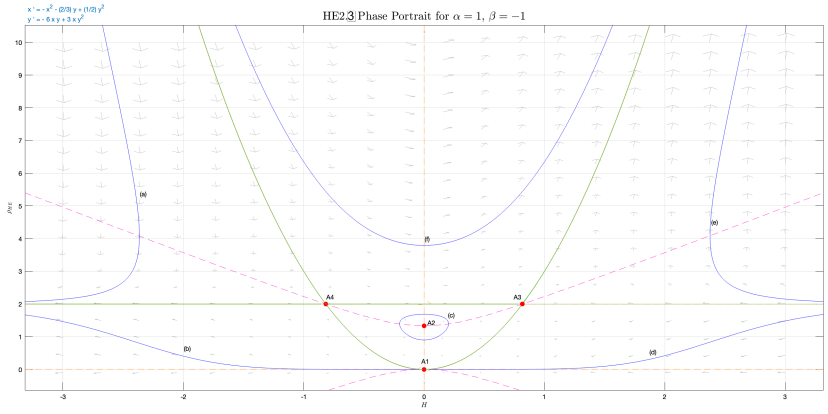


The fixed point A2 reappears, this time with a center-type nature. The behaviour of (a), (b), (d), (e), (f) and the orbits that lie on the separatrices remains the same as it is described for the $HE2.2$ phase portrait. The only difference is for the region to which (c) belongs: these closed non-phantom models evolve as concentric orbits around A2, which is a generalized static Einstein model. Orbits of this kind contract and expand periodically for infinity while the energy density decreases and increases correspondingly, the reversal of the trend is met on the intersections with the vertical nullcline, on which the maximum and minimum values of $\rho_{HE}$ and of $H$ are reached.

# Low Energy Regime

In the low energy approximation the quadratic term in (25) becomes neglectable in comparison to the linear and the constant terms, the EoS takes the affine form:

$$P_{LE} = P_0 + \alpha\rho_{LE} \tag{46}$$

Consequently, the fluid equation becomes:

$$\dot{\rho}_{LE} = -3\frac{\dot{a}}{a}[P_0 + \rho_{LE}(\alpha + 1)] \tag{47}$$

As we have done for the high energy regime, we can integrate (47) to obtain the following functional expression of the energy density:

$$\rho_{LE}(a) = \begin{cases} \rho_0 - 3P_0 \ln\left(\frac{a}{a_0}\right), & \text{if} \quad \alpha = -1 \\ -\frac{P_0}{\alpha+1} + \left[\rho_0 + \frac{P_0}{\alpha+1}\right]\left(\frac{a}{a_0}\right)^{3(\alpha+1)}, & \text{if} \quad \alpha \neq -1 \end{cases} \tag{48}$$

Here we have called $\rho_0 \equiv \rho(t = 0)$ and $a_0 \equiv a(t = 0)$, where $t_0$ is the arbitrary instant of time from which we started integrating. As we did before, since we are interested in the more general case, we will study the energy density under the condition $\alpha \neq -1$. To make the function more clear we can define $\tilde{\rho}_\Lambda \equiv -P_0/(\alpha + 1)$, so that:

$$\rho_{LE}(a) = \tilde{\rho}_\Lambda + (\rho_0 - \tilde{\rho}_\Lambda)\left(\frac{a}{a_0}\right)^{3(\alpha+1)} \tag{49}$$

From (46) we immediately see that $\tilde{\rho}_\Lambda$ defines an effective cosmological constant and it is positive only if $P_0/(1 + \alpha) < 0$. From this standpoint, we will start by looking at the case in which $\tilde{\rho}_\Lambda$ doesn't define an effective cosmological constant, we will then look at when an effective cosmological constant is present. In the latter scenario, since $\tilde{\rho}_\Lambda$ falls in the physical region of the phase space ($\rho_{LE} > 0$), we will find the two possibilities $\rho_{LE} < \tilde{\rho}_\Lambda$ and $\rho_{LE} > \tilde{\rho}_\Lambda$. The tree cases are:

1. $D$: $\tilde{\rho}_\Lambda < 0$

   Here we can rewrite (49) in a more insightful form:

   $$\rho_{LE}(a) = -|\tilde{\rho}_\Lambda| + (\rho_0 + |\tilde{\rho}_\Lambda|)\left(\frac{a}{a_0}\right)^{3(\alpha+1)} \tag{50}$$

   Imposing $\rho_{LE}(a) > 0$ we see that all values of $a$ are possible in this range of $\tilde{\rho}_\Lambda$, in fact it is implied that:

   $$\left(\frac{a}{a_0}\right)^{3(\alpha+1)} > \frac{|\tilde{\rho}_\Lambda|}{\rho_0 + |\tilde{\rho}_\Lambda|} > 0 \tag{51}$$

   So $0 < a < \infty$. Again, the $\tilde{\rho}_\Lambda < 0$ range is obtained under two possible conditions:

- *D1*: $P_0 > 0$ and $\alpha > -1$. Under these constraints the energy density range is $-|\tilde{\rho}_\Lambda| < \rho_{LE} < \infty$, in fact for $a \to \infty$ we have $\rho_{LE} \to \infty$ and for $a \to 0$ we have $\rho_{LE} \to -|\tilde{\rho}_\Lambda|$. As we will see in the phase portraits that follow, the exact behaviour of these kind of solutions is better defined taking into consideration the geometry of the universe. In detail, the open models cannot be regarded as physical, as the evolution includes (either in the past or in the future) portions of the phase space with negative energy density. Flat solutions start by expanding until a stationary point is met - in correspondence of a null energy density - then the trend reverses and a contraction takes place. The same happens for the closed models in two of the subcases, except that the maximum $a$ is reached at a generic minimum of $\rho_{LE}$. The difference happens for closed models in the $-1 < \alpha < -1/3$ range, where an infinite cycle of contractions and expansions around the center B1 takes place, in this case the scale factor is clearly limited both superiorly and inferiorly.
- *D2*: $P_0 < 0$ and $\alpha < -1$. For $a \to \infty$ we have $\rho_{LE} \to -|\tilde{\rho}_\Lambda|$ and for $a \to 0$ we have $\rho_{LE} \to \infty$. Again, $-|\tilde{\rho}_\Lambda| < \rho_{LE} < \infty$. Here open models are nonphysical, because they reach the negative energy density portion of the phase space. Flat and closed solutions are characterized by a bounce: at first a contraction takes place, a minimum of $a$ is reached - with minimum $\rho_{HE}$: 0 for flat models, nonzero for closed ones - then the expansion starts and goes on. As we can notice, in this range the fluid has phantom behaviour.

2. *E*: $\tilde{\rho}_\Lambda > 0$ and $\rho_{LE} > \tilde{\rho}_\Lambda$

   The energy density can be written as:

$$\rho_{LE}(a) = \tilde{\rho}_\Lambda + |\rho_0 - \tilde{\rho}_\Lambda| \left(\frac{a}{a_0}\right)^{3(\alpha+1)} \tag{52}$$

   Again, $0 < a < \infty$. There are two ways to satisfy $\tilde{\rho}_\Lambda > 0$:

   - *E1*: $P_0 > 0$ and $\alpha < -1$. Calculating the relevant limits in the range of the scale factor, we see that for the energy density is valid $\tilde{\rho}_\Lambda < \rho_{LE} < \infty$. The closed models behave as in *D2* and each one of the solutions in this subset is a phantom one. Open models are asymptotical to $\rho_{LE} = \tilde{\rho}_\Lambda$ in the past/future, approaching/leaving a phase in which $\rho_{LE} \to \infty$ as well as $a \to \infty$. The same happens for flat models, with the only difference that solutions fall off/into the equilibriums B2/B3[29].
   - *E2*: $P_0 < 0$ and $\alpha > -1$. The range for the energy density remains $\tilde{\rho}_\Lambda < \rho_{LE} < \infty$. The fluid is standard, here open and flat solutions are all asymptotical to the phantom separatrix $\rho_{LE} = \tilde{\rho}_\Lambda$ while coming from Big Bang/Big Crunch singularities. The closed ones have a bounce behaviour, in that they leave or arrive to a flat universe (in the fixed points), reaching a maximum energy density in correspondence of a minimum of the scale factor.

3. *F*: $\tilde{\rho}_\Lambda > 0$ and $\rho_{LE} < \tilde{\rho}_\Lambda$

   Here we can write:

$$\rho_{LE}(a) = \tilde{\rho}_\Lambda - |\rho_0 - \tilde{\rho}_\Lambda| \left(\frac{a}{a_0}\right)^{3(\alpha+1)} \tag{53}$$

   Equally as before, we find that in general $0 < a < \infty$, and as we found in $E$ we have two subcases:

   - *F1*: $P_0 > 0$ and $\alpha < -1$. Here the range for the energy density is $-\infty < \rho_{LE} < \tilde{\rho}_\Lambda$. Once again open models aren't acceptable because they do not satisfy $\rho_{LE} > 0$ for all the times. The closed models revolve in closed loops about an Einstein universe solution (fixed point), alternating

[29] See the linear stability analysis that follows.

moments of expansion with moments of contraction, which implies that the range of $a$ is limited by a maximum and a minimum. Lastly, flat models leave a de Sitter universe (expanding, fixed energy density), pass through a static universe with null energy density (Minkowski) and then return towards a contracting de Sitter solution. The behaviour is non-phantom for every orbit.

- *F2*: $P_0 < 0$ and $\alpha > -1$. Here the range remains the same: $-\infty < \rho_{LE} < \tilde{\rho}_\Lambda$, but as we have seen in the other cases (*D*, *E*) these significant limits are obtained inverting the extremal points of $a$ in respect to the cases "1"[30]. The open models are not physical, the closed and flat ones are asymptotical to $\rho_{LE} = \tilde{\rho}_\Lambda$ (de Sitter) both in the past and in the future, portraying a phantom bounce.

## 0.12 Preliminary stability analysis: low energy regime

If we look at the dynamical system given by the fluid equation together with the Raychaudhuri equation, imposing (46) we have:

$$\begin{cases} \dot{\rho}_{LE} = -3H[P_0 + \rho_{LE}(\alpha+1)] \\ \dot{H} = -H^2 - \frac{1}{6}[3P_0 + \rho_{LE}(3\alpha+1)] \end{cases} \tag{54}$$

The fixed points, where both first derivatives of $\rho_{LE}$ and $H$ are zero, together with their existence conditions, are:

| Name | $\rho_{LE}$ | $H$ | Existence |
|---|---|---|---|
| B1 | $-\frac{3P_0}{3\alpha+1}$ | $0$ | $\frac{P_0}{3\alpha+1} < 0$ |
| B2 | $-\frac{P_0}{\alpha+1}$ | $+\sqrt{-\frac{P_0}{3(\alpha+1)}}$ | $\frac{P_0}{\alpha+1} < 0$ |
| B3 | $-\frac{P_0}{\alpha+1}$ | $-\sqrt{-\frac{P_0}{3(\alpha+1)}}$ | $\frac{P_0}{\alpha+1} < 0$ |

As done in the previous chapter, the existence is established by imposing a positive energy density and that the fixed points must be real numbers. When it exists, B1 represents a model for a generalized Einstein universe, that is a static one with fixed nonzero energy density. On the other hand, when B2 and B3 are present they are respectively expanding and contracting de Sitter models, namely flat universes with nonzero energy density. The Jacobian matrix of the dynamical system reads:

$$J_X^{LE}(\rho_{LE}, H) = \begin{bmatrix} -3H(\alpha+1) & -3P_0 - 3\rho_{LE}(\alpha+1) \\ -\frac{3\alpha+1}{6} & -2H \end{bmatrix} \tag{55}$$

The eigenvalues of the matrix, evaluated in the fixed points $B_i$, are:

| Fixed point | $\lambda_1(B_i)$ | $\lambda_2(B_i)$ |
|---|---|---|
| B1 | $\sqrt{-P_0}$ | $-\sqrt{-P_0}$ |
| B2 | $\sqrt{-\frac{3(\alpha+1)}{P_0}}$ | $-\frac{2}{\sqrt{-3P_0(\alpha+1)}}$ |
| B3 | $-\sqrt{-\frac{3(\alpha+1)}{P_0}}$ | $\frac{2}{\sqrt{-3P_0(\alpha+1)}}$ |

To gain information on the nature of the fixed points, we will look at the cases that give rise to different behaviours, according to the techniques of stability analysis presented in the first chapter. A main factor is the sign of the constant pressure term, $P_0$, which gives an instant categorization for B1. Once that is established, different subcases arise by choosing the range of $\alpha$, fixing the nature of B2 and B3.

[30] Essentially, as we found before, the limits remain the same but the trend is inverted. In *F2*, for example, $\tilde{\rho}_\Lambda$ is obtained when $a \to 0$, whilst in *F1* it is found for $a \to \infty$.

## 0.13 $LE1$: $P_0 > 0$

With a positive constant pressure term, the point B1 - which is the solution for a generalized Einstein universe (static, fixed nonzero energy density) - gives eigenvalues which are both purely imaginary: this makes B1 a center. Existence for B1 is granted only if $\alpha < -\frac{1}{3}$, otherwise the equilibrium won't be present. B2 and B3 are saddles if they are real numbers, that is if $\alpha < -1$; with $P_0 > 0$ this is also their existence condition, so here B2 and B3 do not exist for $\alpha > -1$. It is interesting to note that for $\alpha \geq -1/3$ no fixed points are found. To sum it up, in this case the nature of the fixed points is as follows:

| Fixed point | Stability |
|---|---|
| B1 | Center if $\alpha < -\frac{1}{3}$ and $\nexists$ otherwise |
| B2 | Saddle if $\alpha < -1$ and $\nexists$ otherwise |
| B3 | Saddle if $\alpha < -1$ and $\nexists$ otherwise |

We will now proceed by looking at the three subcases that arise from the existence conditions of the equilibriums:

- $LE1.1$: $\alpha < -1$. We set $P_0 = 1$ and $\alpha = -2$ to obtain the following phase portrait:

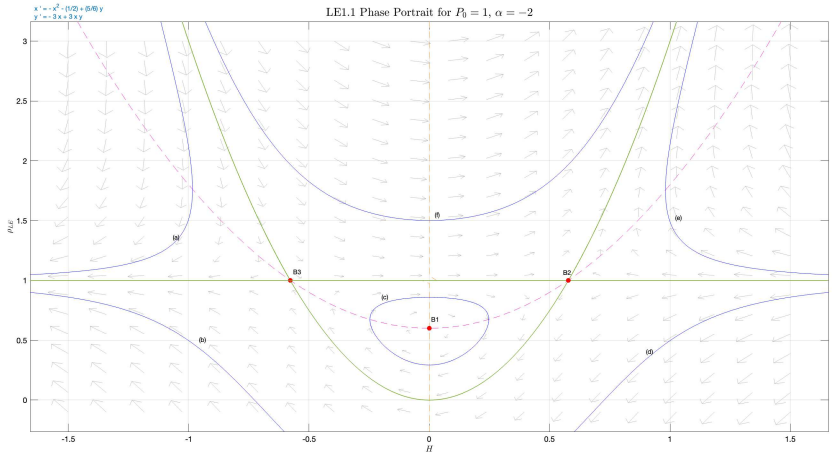


The horizontal line intersecting B2 and B3, namely $\tilde{\rho}_\Lambda = P_0/(1+\alpha)$, is the phantom separatrix. As we can see, for $\rho_{LE} > \tilde{\rho}_\Lambda$ the fluid behaves in a phantom manner (subcase *E1*), in that the energy density decreases for a contracting universe and vice versa for an expanding one. On the other side, for $\rho_{LE} < \tilde{\rho}_\Lambda$ the fluid behaves in a standard manner (*F1*). The orbits (a), (b) (d) and (e) represent open models. (a) is a phantom model and it evolves from a Type I singularity in the past whilst approaching the phantom separatrix in the future, that is a contracting universe with fixed energy density. (e) is the exact symmetric of (a) under time reversal. (b) and (d) have to be excluded because they are nonphysical, in fact in their evolution they enter the prohibited domain $\rho_{LE} < 0$. (c) and (f) represent closed models: (c) behaves in a standard manner, it undergoes alternating phases of expansion/contraction to a maximum/minumum $a$; (f) starts and ends in a Typy I singularity, undergoing at first a contraction - to a minimum $a$ - and then an expansion (phantom bounce). The (c)-type orbits are distributed concentrically about the static Einstein universe in B1. The other two fixed points are de Sitter universes and they lie on the parabola for flat models: in the standard region these models evolve leaving B2 and going towards B3 in the future, on the phantom separatrix they evolve leaving B3/approaching B2 in both directions and in the phantom region the left branch of the parabola starts from a Type I singularity and approaches B3 in the future, whilst the right one leaves B2 to reach the same type of singularity.

- $LE1.2$: $-1 < \alpha < -\frac{1}{3}$. For the following phase portrait we have set $P_0 = 1$ and $\alpha = -2/3$:

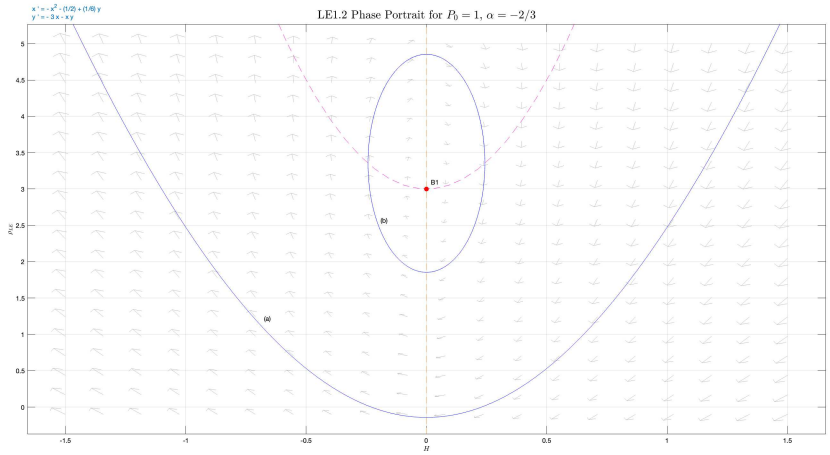


Here the phantom separatrix is absent, along with B2 and B3 which do not exist. All models behave in a standard way ($D1$), but no one of them is physical: the open ones have to be discarded because their evolution enters the $\rho_{LE} < 0$ region. Closed models, as (b), oscillate between a maximum and minum $a$ around the fixed point B1. Flat models lie on the separatrix (a) and evolve from a standard Big Bang to a standard Big Crunch, with a Minkowski universe as interlude (in the vertex of the parabola, with $H = 0$ and $\rho_{LE} = 0$).

- $LE1.3$: $\alpha \geq -\frac{1}{3}$. By setting $P_0 = 1$ and $\alpha = 1$ we obtain:

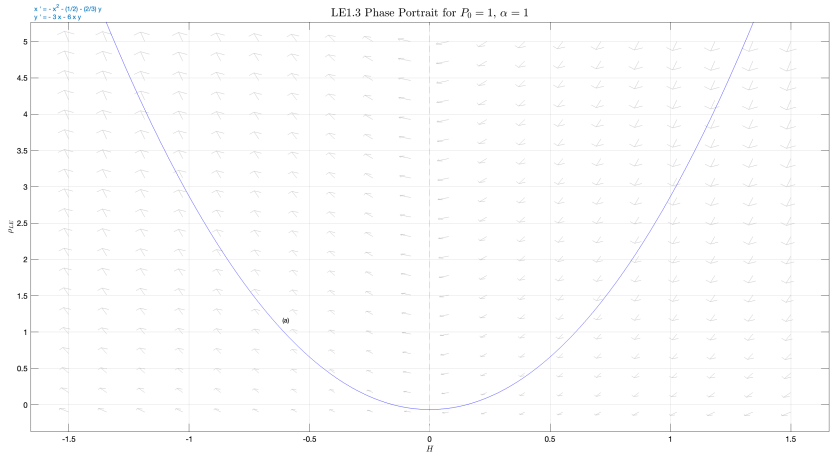


Here, except for closed models, the behaviour is similar to $LE1.2$. The fluid is standard in all the phase space ($D1$) and open models are nonphysical because they reach $\rho_{LE} < 0$. There is a total absence of fixed points, for their existence conditions are not met in this subcase. Closed models start from standard Big Bang, evolve to a maximum $a$ and recollapse in a standard Big Crunch. Flat models are a specific case of this behaviour for that, as in $LE1.2$, they reach a Minkowski universe before recollapsing.

## 0.14 $LE2$: $P_0 < 0$

The negative constant pressure term makes the root in the eigenvalues for B1 real, because of this the point assumes a saddle nature. On the other side, when the existence conditions for B2/B3 are met, they

exhibit attractor/repeller nature. Here there are no fixed points for $\alpha < -1$. In total:

| Fixed point | Stability |
|---|---|
| B1 | Saddle if $\alpha \geq -\frac{1}{3}$ and $\nexists$ otherwise |
| B2 | Attractor if $\alpha > -1$ and $\nexists$ otherwise |
| B3 | Repeller if $\alpha > -1$ and $\nexists$ otherwise |

- $LE2.1$: $\alpha < -1$. Fixing $P_0 = -1$ and $\alpha = -2$ the following phase portrait is obtained:

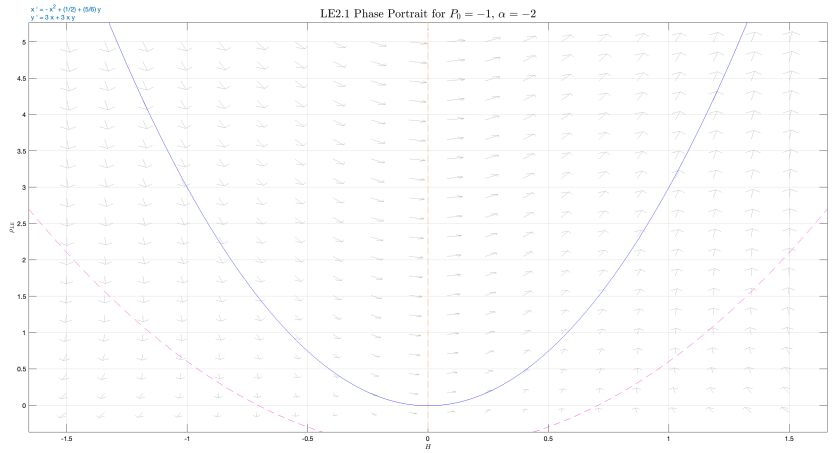


The fluid behaves in a phantom manner (subcase *D2*) in all of the physical portion of the phase space and no fixed points exist. As we found in other of the previous subcases, trajectiories beneath the separatrix for open and closed models, i.e. the orbit for flat models, are nonphysical. This means that in this scenario all open models have to be discarded. Similarly to $LE1.3$, closed and flat models evolve leaving and approaching a Type I singularity, with an intermediate phase in which a stationary point for $a$ (a minimum) is reached, in this context the behaviour is dubbed as "phantom bounce". For the flat model the minimum corresponds to a Minkowski universe.

- $LE2.2$: $-1 < \alpha < -\frac{1}{3}$. For the phase portrait below we have set $P_0 = -1$ and $\alpha = -2/3$:

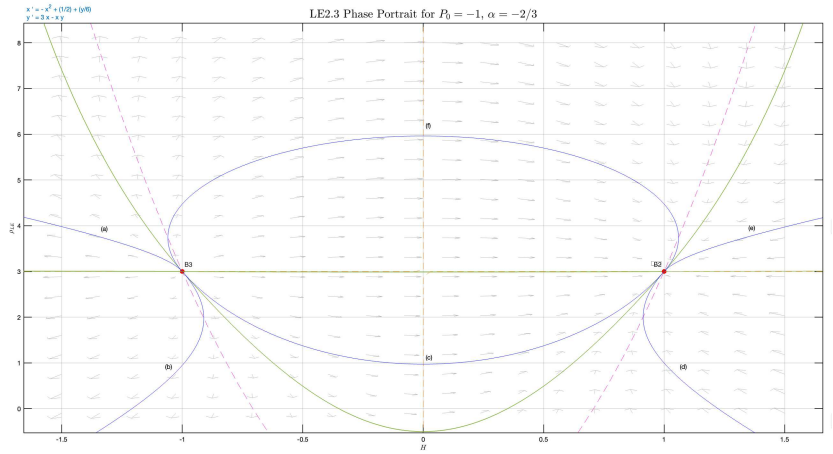


The fixed points B2 and B3 reappear, respectively as attractor and as repeller. The phantom region lies underneath the phantom separatrix that connects horizontally the equilibriums. The solutions (a), (b), (d) and (e) have negative curvature (open universes); (b) and (d) are nonphysical whilst (a)

leaves a flat universe (in B3) towards a Big Crunch and (e) comes from a Big Bang and approaches a flat expanding universe (in B2), the latter both portray a standard behaviour. On the other hand, (c) and (f) are closed models, the first one is phantom, the second is standard: they evolve by contracting and leaving the flat B3 solution, in order to re-expand to B2 in the future. During their evolution a minimum in the scale factor is achieved, the only difference being that in (f) the minimum happens in the maximum of $\rho_{LE}$ whilst in (c) it happens for its minimum, as expected. Speaking about the flat universe solutions: two of them are the fixed points B2 (stable) and B3 (unstable); the lower part of the parabola in green (phantom) defines a contraction that starts with the solution leaving B3 - a Minkowski universe is then reached - and ends with an expansion towards B2; the left upper branch represents a contraction towards a Big Crunch, on the flipside the right one evolves from a Big Bang towards the fixed expansion rate and energy density in B2.

- $LE2.3$: $\alpha \geq -\frac{1}{3}$. The phase portrait below is obtained by imposing $P_0 = -1$ and $\alpha = -2/3$:

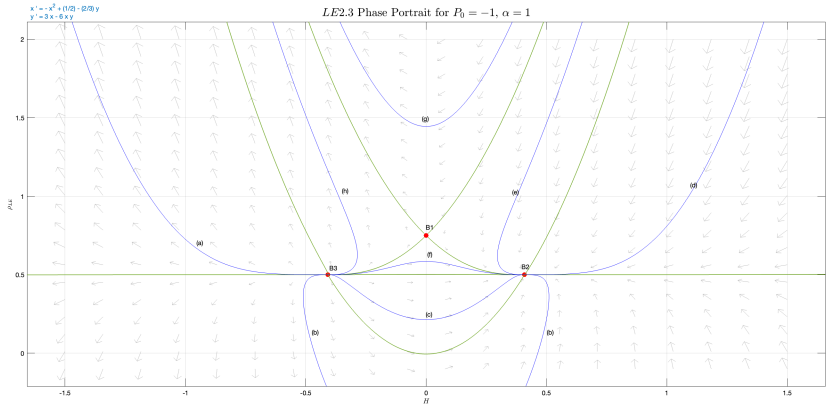


In this subcase the three possible fixed points are all present and they behave as previously stated. B2 and B3 lie on the intersection between the phantom separatrix $\rho_{LE} = \tilde{\rho}_\Lambda$ and the parabola for flat models given by the Friedmann equation with zero curvature term. The phantom region lies below the phantom separatrix, whilst the standard region is above it. (a), (b) and (d) are open models, the (b)-type solutions are nonphysical and have to be excluded for the same reasons stated in the other subcases. (a) evolves leaving a flat de Sitter universe (in B3) and contracting until a standard Big Crunch singularity is reached, (d) behaves symmetrically as it leaves a standard Big Bang singularity in the past whilst approaching the flat expanding de Sitter universe in B2. The orbits (c), (e), (f), (g), (h) represent closed universes and the only one of them that behaves in a phantom manner is (c). (c) leaves B3 and contracts to a minimum $a$ (minimum $\rho_{LE}$), then re-expands towards the flat expanding de Sitter universe in B2. The (f) orbit is similar to the (c) one (bounce models), apart from the fact that it represents a standard fluid, so that the minimum of the scale factor is achieved in correspondence of the energy density maximum. (e) represents closed standard solutions that evolve leaving a Big Bang singularity and approaching B2 in the future, likewise (h) leaves B2 and goes towards a standard Big Crunch. The (g)-type solution is a turn-around model as it evolves from a past Big Bang, it expands reaching a minimum of the energy density and finally it recollapses into a Big Crunch singularity. The orbits on the phantom separatrix are attracted by B2 and repelled by B3, in detail, starting from left to right: the first one leaves B3 whilst approaching a Big Crunch, the second one moves away from B3 towards B2 and the third one evolves from a Big Bang to reach B2 in the future; in each case the energy density of the universe remains fixed.

# Full Equation of State

We will now consider the full quadratic equation of state:

$$P(\rho) = P_0 + \alpha\rho + \beta\rho^2 \tag{56}$$

For which the fluid equation now reads:

$$\dot{\rho} = -3H[P_0 + (\alpha + 1) + \beta\rho^2] \tag{57}$$

To obtain a functional form for the energy density, we need to integrate:

$$\int_{t_0}^{t} \frac{1}{[P_0 + (\alpha+1)\rho + \beta\rho^2]} \frac{\partial\rho}{\partial t'} dt' = -3 \int_{t_0}^{t} \frac{1}{a} \frac{\partial a}{\partial t'} dt' \tag{58}$$

Which gives:

$$\left. \frac{2 \arctan\left(\frac{2\beta\rho+\alpha+1}{\sqrt{\Delta}}\right)}{\sqrt{\Delta}} \right|_{t_0}^{t} = -3 \ln\left(\frac{a}{a_0}\right) \tag{59}$$

Here $\Delta \equiv (\alpha+1)^2 - 4\beta P_0$ is the discriminant of the quadratic denominator in the left term of (58). It is also directly connected to the presence of an effective cosmological constant, in fact $P(\rho_\Lambda) = -\rho_\Lambda$ gives the same equation for which $\Delta$ is the discriminant. This suggests that three different scenarios may occur: we will have two effective cosmological points if $\Delta > 0$, one if $\Delta = 0$ and none if $\Delta < 0$ (no real solution is admitted). When they exist these points are:

$$\rho_{\Lambda,1} \equiv \frac{-(\alpha+1) + \sqrt{\Delta}}{2\beta} \quad \text{and} \quad \rho_{\Lambda,2} \equiv \frac{-(\alpha+1) - \sqrt{\Delta}}{2\beta} \tag{60}$$

The presence of $\rho_{\Lambda,1/2}$ depends on the range of $\Delta$ as much as the solutions of (59) do. Due to this, we will present the latter in the context of the three main cases that arise based on the discriminant:

1. *G*: $\Delta < 0$

   In this case the energy density assumes the form:

   $$\rho = \frac{\Gamma - \sqrt{|\Delta|} \tan\left[\frac{3}{2}\sqrt{|\Delta|} \ln\left(\frac{a}{a_0}\right)\right]}{2\beta + \frac{2\beta}{\sqrt{|\Delta|}}\Gamma \tan\left[\frac{3}{2}\sqrt{|\Delta|} \ln\left(\frac{a}{a_0}\right)\right]} \tag{61}$$

   Having defined $\Gamma \equiv 2\beta\rho_0 + (\alpha+1)$.

   - *G1*: $\beta > 0$ and $P_0 > 0$. The scale factor has an upper and lower bound, namely $a_1 < a < a_2$. This leaves the energy density with no limits whatsoever and, being the behaviour in this subset standard, the minimum/maximum of $\rho$ are reached for the maximum/minimum of $a$. The open

models of this subset are all to be disregarded: their evolution enters the prohibited $\rho < 0$ region. Closed models can behave in a loop manner, oscillating infinitely in a limited portion of the phase space, or reach a maximum $a$ (minimum $\rho$) and recollapse, this happens also to the flat models in this subset (for which $\min\{\rho\} = 0$).

- *G2*: $\beta > 0$ and $P_0 > 0$. The scale factor is limited, as it was in *G1*, but the behaviour of the fluid is phantom, this means that the maximum $\rho$ is reached in correspondence to the maximum $a$ and the same for the minimums. The open solutions in this subset are nonphysical, the flat and closed ones are turn-around models.

2. *H*: $\Delta = 0$

In this case a single effective cosmological constant point is present, that is $\bar{\rho} \equiv \rho_{\Lambda,1} = \rho_{\Lambda,2}$, leading to:

$$\rho = \bar{\rho}_\Lambda + \frac{1}{3\beta \ln\left(\frac{a}{a_0}\right) + \frac{2\beta}{\Gamma}} \tag{62}$$

The fact that $\bar{\rho}_\Lambda \in \mathbb{R}$ does not mean that such point is present in the phyisical region of the phase space, meaning that such thing happens only if $\bar{\rho}_\Lambda > 0$.

- *H1*: $\beta > 0$, $P_0 > 0$ and $\rho < \bar{\rho}_\Lambda$. With this subset of conditions we have $0 < a < a_1$, the energy density is upperly bound by the effective cosmological constant ($-\infty < \rho < \bar{\rho}_\Lambda$) and the behaviour of the fluid is standard, so that maxima and minima of $a$ and $\rho$ occur accordingly. Open models are nonphysical; flat models expand from one de Sitter point (in $H > 0$) and re-contract to the symmetrical one (in $H < 0$), the maximum for $a$ is reached in correspondence with the origin ($H = 0, \rho = 0$) of the phase space; closed models evolve in infinite concentric loops around a static generalized Einstein universe.

- *H2*: $\beta > 0$, $P_0 > 0$ and $\rho > \bar{\rho}_\Lambda$. The fluid still exhibits standard behaviour, but here $a_1 < a < \infty$ and $\bar{\rho}_\Lambda < \rho < \infty$ which means that a Type III singularity is possibly admitted as an attractor in the future/past. The behaviour of the solutions depends on wether $\bar{\rho}_\Lambda$ is physical ($> 0$) or not ($< 0$). If $\bar{\rho}_\Lambda > 0$ all open and flat models start/end in the singularity and end/start in the expanding/contracting fixed generalized de Sitter points; closed models either undergo a bounce and turn-around (starting and ending in the singularity) or they start and end in the generalized de Sitter fixed points, two solutions can also start/end in a generalized Einstein universe and end/start in a generalized de Sitter point. If $\bar{\rho}_\Lambda < 0$ the open models enter the prohibited region in their evolution, whilst flat and open ones undergo a recollapse.

- *H3*: $\beta < 0$, $P_0 < 0$ and $\rho < \bar{\rho}_\Lambda$. Here $a_1 < a < \infty$ and $-\infty < \rho < \bar{\rho}_\Lambda$, with a correspondence of maxima/minima for $a$ and $\rho$, because of the phantom behaviour that is met with this subset of conditions. The open models are nonphysical, the flat end closed ones leave a contracting generalzied de Sitter fixed point and approach an expanding one in the future.

- *H4*: $\beta < 0$, $P_0 < 0$ and $\rho > \bar{\rho}_\Lambda$. Here $0 < a < a_1$ and $\bar{\rho}_\Lambda < \rho < \infty$, the behaviour of the fluid is phantom and the presence of a past/future singularity is a general feature of the solutions. However, if $\bar{\rho}_\Lambda < 0$, during their evolution the open models always enter the negative energy density portion of the phase space, hence they are nonphysical. Closed models always undergo a phantom bounce, whilst if $\bar{\rho}_\Lambda > 0$ the flat and open ones approach or leave, on one extreme of the orbit, a contracting or expanding phase with $\rho \to \bar{\rho}_\Lambda$.

3. *I*: $\Delta > 0$

Here we have $\rho_{\Lambda,1} \neq \rho_{\Lambda,2}$ and:

$$\rho = \frac{\rho_{\Lambda,2}\left(\frac{a}{a_0}\right)^{-3\sqrt{\Delta}} - \rho_{\Lambda,1}C}{\left(\frac{a}{a_0}\right)^{-3\sqrt{\Delta}} - C} \tag{63}$$

Having set $C \equiv \frac{\rho_0 - \rho_{\Lambda,2}}{\rho_0 - \rho_{\Lambda,1}}$. The parameter $\beta$ influences the effective cosmological points in that for $\beta > 0$ we have $\rho_{\Lambda,1} > \rho_{\Lambda,2}$, for $\beta < 0$ we have $\rho_{\Lambda,1} < \rho_{\Lambda,2}$. The sign of $C$ is also influent in determining in which region $\rho_0$ falls, but it won't be relevant for our present considerations, in which we give general descriptions of all the possible regions. For physical reasons we assume that both the effective cosmological constant points are positive for the following subdivision:

- *I1*: $\beta > 0$, $P_0 > 0$ and $\rho < \rho_{\Lambda,2}$. We implicitly assume $\rho_{\Lambda,2} > 0$, otherwise we would not have any physical solutions with this subset of conditions. Here we have an upper limit for the scale factor, $0 < a < a_1$, and $-\infty < \rho < \rho_{\Lambda,2}$. The behaviour is standard, so that $\rho \overset{a\to a_1}{\to} -\infty$ and vice versa $\rho \overset{a\to 0}{\to} \rho_{\Lambda,2}$. Open models are nonphysical, they all evolve to $\rho < 0$. Flat models evolve from a contracting generalized de Sitter point to an expanding one, one closed solution does the same whilst the other ones loop infinitely - between maximums and minimums of $a$ and $\rho$ - around a generalized Einstein universe (also closed).

- *I2*: $\beta > 0$, $P_0 > 0$ and $\rho_{\Lambda,2} < \rho < \rho_{\Lambda,1}$. Here $0 < a < \infty$ and obviously $\rho_{\Lambda,2} < \rho < \rho_{\Lambda,1}$, the fluid in this subset is phantom and maximums/minimums behave accordingly. Open models leave/approach a contracting/expanding de Sitter fixed point and approach/leave $\rho_{\Lambda,2}$. Flat models evolve from one contracting de Sitter point to another, or from an expanding one to another. Closed models move from a contracting de Sitter point to an expanding one, reaching a minimum $a$ in the middle of their evolution.

- *I3*: $\beta > 0$, $P_0 > 0$ and $\rho > \rho_{\Lambda,1}$. Here $0 < a < \infty$ and $\rho_{\Lambda,1} < \rho < \infty$, the behaviour is standard. A Type III singularity in the past/future is a general feature in most of the models in this subset. Open and flat ones are asymptotical to either contracting or expanding generalized flat de Sitter points. Closed models can either undergo a standard bounce (after an expansion) and contract back to the singularity, or they can evolve from one contracting de Sitter point to an expanding one, else they are linked to a generalized Einstein universe in some way. In the latter case they start/end in the singularity or in one of the de Sitter fixed points.

- *I4*: $\beta < 0$, $P_0 < 0$ and $\rho < \rho_{\Lambda,1}$. In this subset we have $a_1 < a < \infty$ and $-\infty < \rho < \rho_{\Lambda,2}$, the fluid exhibits phantom behaviour. Open models are nonphysical, flat ones and closed ones evolve from a contracting generalized de Sitter flat point to an expanding one. Both flat and closed models reach a minimum for $a$ and $\rho$ (together) in their evolution, for the flat case this minimum corresponds to a Minkowski universe: the origin.

- *I5*: $\beta < 0$, $P_0 < 0$ and $\rho_{\Lambda,1} < \rho < \rho_{\Lambda,2}$. Here the energy density is clearly bound by the two effective cosmological constants, whilst the scale factor is unlimited a priori (more constraints are given by the particular class of solutions), so $0 < a < \infty$, the fluid is standard in this scenario. Open models either collapse towards the maximum energy density and minimum scale factor, starting from a flat de Sitter contracting fixed point, or do the exact opposite and they approach the flat de Sitter expanding fixed point. Flat models behave in a similar manner, with the only difference that they move from one fixed point to the other, so the rate at which the expansion/contraction happens is not unlimited. Closed models can contract from one de Sitter fixed point and subsequently expand to another one (with same energy density $\rho = \rho_{\Lambda,1}$), or they can loop infinitely around a generalized Einstein static solution (meaning, as usual, within a limited unchanging range of $a$ and $\rho$), else they are connected to the same Einstein

universe and either start and end on it, or start/end on it and end/start either on a contracting or expanding flat generalized de Sitter universe.

- *I6*: $\beta < 0$, $P_0 < 0$ and $\rho > \rho_{\Lambda,2}$. Here $0 < a < a_1$, $\rho_{\Lambda,2} < \rho < \infty$, hence a past/future singularity is admitted and in fact all models (for all the geometries) have one. The fluid behave in a phantom manner. Open models are, on one extreme, asymptotical to the upper effective cosmological constant energy density, flat ones to, with the only difference that they reach a finite Hubble parameter and their expansion/contraction rate does not increase (in absolute value) indefinitely. On the other extreme of flat and open models there is the singularity. Closed solutions undergo a phantom bounce, hence they are turn-around models, the singularity is found at both extremes of their orbit. The geometry of closed models tends to a flat one in the past and in the future, as it does in all the closed phantom bounce models we saw, the curvature of the open models also tends to zero but either in the past (contracting models) or in the future (expanding models).

## 0.15 Preliminary stability analysis: full EoS

The dynamical system composed by (14) and (6) with the pressure given by (56) is:

$$\begin{cases} \dot{\rho} = -3H[P_0 + (\alpha+1)\rho + \beta\rho^2] \\ \dot{H} = -H^2 - \dfrac{1}{6}[3P_0 + (3\alpha+1)\rho + 3\beta\rho^2] \end{cases} \tag{64}$$

We find seven possible fixed points for the system, this time we meet a much richer variety of existence conditions, which have been found by imposing the reality condition for the square roots and by considering only non-negative values of the energy density:

| Name | $\rho$ | $H$ | Existence for $\beta > 0$ | Existence for $\beta < 0$ |
|---|---|---|---|---|
| C1 | $0$ | $0$ | $P_0 = 0$ | $P_0 = 0$ |
| C2 | $\frac{-(3\alpha+1)+\sqrt{(3\alpha+1)^2-36P_0\beta}}{6\beta}$ | $0$ | $P_0 \leq P_1$, $\alpha < -\frac{1}{3}$ or $P_0 < 0$, $\alpha > -\frac{1}{3}$ | $P_1 < P_0 < 0$, $\alpha > -\frac{1}{3}$ |
| C3 | $\frac{-(3\alpha+1)-\sqrt{(3\alpha+1)^2-36P_0\beta}}{6\beta}$ | $0$ | $0 < P_0 < P_1$, $\alpha < -\frac{1}{3}$ | $P_0 > 0$, $\alpha < -\frac{1}{3}$ or $P_0 \geq P_1$, $\alpha > -\frac{1}{3}$ |
| C4$_\pm$ | $\frac{-(\alpha+1)+\sqrt{(\alpha+1)^2-4P_0\beta}}{2\beta}$ | $\pm\sqrt{\frac{-(\alpha+1)+\sqrt{(\alpha+1)^2-4P_0\beta}}{6\beta}}$ | $P_0 \leq P_2$, $\alpha < -1$ or $P_0 < 0$, $\alpha > -1$ | $P_2 < P_0 < 0$, $\alpha > -1$ |
| C5$_\pm$ | $\frac{-(\alpha+1)-\sqrt{(\alpha+1)^2-4P_0\beta}}{2\beta}$ | $\pm\sqrt{\frac{-(\alpha+1)-\sqrt{(\alpha+1)^2-4P_0\beta}}{6\beta}}$ | $0 < P_0 < P_2$, $\alpha < -1$ | $P_0 > 0$, $\alpha < -1$ or $P_2 \leq P_0$, $\alpha > -1$ |

We see that, when these points exist, they are respectively: $C_1$ a Minkowski universe (present only if $P_0 = 0$), $C_2$ and $C_3$ generalized Einstein universes, $C4_\pm$ and $C5_\pm$ four generalized de Sitter universes (expanding for the $+$, contracting for the $-$). In addition, we note how the conformation of the phase space is strongly influenced by the range of the constant pressure term $P_0$, for which we defined:

$$P_1 \equiv \frac{(3\alpha+1)^2}{36\beta}, \qquad P_2 \equiv \frac{(\alpha+1)^2}{4\beta} \tag{65}$$

These two values - as well as the sign of $P_0$ - are significant factors in the characterization of the topology. The Jacobian of the system reads:

$$J_X(\rho, H) = \begin{bmatrix} -3H[(\alpha+1) + 2\beta\rho] & -3[P_0 + (\alpha+1)\rho + \beta\rho^2] \\ -\frac{3\alpha+1}{6} - \beta\rho & -2H \end{bmatrix} \tag{66}$$

The eigenvalues of the matrix, evaluated in the fixed points $C_i$, are:

| Fixed point | $\lambda_1(C_i)$ | $\lambda_2(C_i)$ |
|---|---|---|
| C1 | 0 | 0 |
| C2 | $\sqrt{\frac{\gamma_1^2-\gamma_1\sqrt{\gamma_1^2-36P_0\beta}-36P_0\beta}{18\beta}}$ | $\sqrt{\frac{\gamma_1^2-\gamma_1\sqrt{\gamma_1^2-36P_0\beta}-36P_0\beta}{18\beta}}$ |
| C3 | $\sqrt{\frac{\gamma_1^2+\gamma_1\sqrt{\gamma_1^2-36P_0\beta}-36P_0\beta}{18\beta}}$ | $-\sqrt{\frac{\gamma_1^2+\gamma_1\sqrt{\gamma_1^2-36P_0\beta}-36P_0\beta}{18\beta}}$ |
| $C4_\pm$ | $\mp\sqrt{\frac{\delta-\gamma_2}{6\beta}}(1+\frac{3\delta}{2})+\sqrt{\frac{6\delta^2(3\delta-3\gamma_2-4)+8(\gamma_2(3\delta-1)+\delta)}{48\beta}}$ | $\mp\sqrt{\frac{\delta-\gamma_2}{6\beta}}(1+\frac{3\delta}{2})-\sqrt{\frac{6\delta^2(3\delta-3\gamma_2-4)+8(\gamma_2(3\delta-1)+\delta)}{48\beta}}$ |
| $C5_\pm$ | $\pm\sqrt{\frac{-(\delta+\gamma_2)}{6\beta}}(\frac{3\delta}{2}-1)+\sqrt{-\frac{6\delta^2(3\delta+3\gamma_2+4)+8(\gamma_2(3\delta+1)+\delta)}{48\beta}}$ | $\pm\sqrt{\frac{-(\delta+\gamma_2)}{6\beta}}(\frac{3\delta}{2}-1)-\sqrt{-\frac{6\delta^2(3\delta+3\gamma_2+4)+8(\gamma_2(3\delta+1)+\delta)}{48\beta}}$ |

Here we defined $\gamma_1 \equiv 3\alpha+1$, $\gamma_2 \equiv \alpha+1$, $\delta \equiv \sqrt{(\alpha+1)^2-4P_0\beta} = \sqrt{\gamma_2^2-4P_0\beta}$ in order to simplify the expressions. We note that the sign of $\beta$ this time is not influential in regards to the nature of the fixed points, hence we can sum up the linear stability of the latter before considering the various cases:

| Fixed point | Stability |
|---|---|
| C1 | Undefined |
| C2 | Saddle for $\gamma_1^2 \neq 36P_0\beta$ and undefined otherwise |
| C3 | Center for $\gamma_1^2 \neq 36P_0\beta$ and undefined otherwise |
| $C4_+$ | Attractor for $\gamma_2^2 \neq 4P_0\beta$ and undefined otherwise |
| $C4_-$ | Repeller for $\gamma_2^2 \neq 4P_0\beta$ and undefined otherwise |
| $C5_+$ | Saddle for $\gamma_2^2 \neq 4P_0\beta$ and undefined otherwise |
| $C5_-$ | Saddle for $\gamma_2^2 \neq 4P_0\beta$ and undefined otherwise |

Here the stability nature of the points is given implicitly intending that their existence conditions are met. Now, for the analysis that follows, we will subdivide in the two cases $\beta > 0$ ($EoS1$) and $\beta < 0$ ($EoS2$), with the logic of the two previous chapters. We will then follow the same procedural scheme used by Ananda and Bruni in [1], that is: the qualitatively relevant phase portraits will be presented extensively, these satisfy limited subsets of conditions for $P_0$ and $\alpha$ and their importance is due to the fact that they differ qualitatively from the phase portraits we already found in the other chapters. Before doing so, for $EoS1$ and $EoS2$ separately, a table that reunites all the other possible subcases and that specifies their qualitative similarities (to the phase portraits shown in the script) will be shown. This is done because, apart from quantitative differences in the parameters, that are not fundamental for our analysis, there are a limited number of possible topologies that the phase spaces may assume and our aim is to discuss these type of diverse scenarios.

## 0.16 $EoS1$: $\beta > 0$

The subcases for which the phase portraits are qualitatively similar to those we already met or to those we will meet in the following paragraphs - with reference to these - are reported in the table below:

| | $\alpha < -1$ | $-1 \leq \alpha < -2/3$ | $-2/3 \leq \alpha < -1/3$ | $-1/3 \leq \alpha$ |
|---|---|---|---|---|
| $P_0 > P_1$ | $LE1.3$ | $LE1.3$ | $LE1.3$ | $LE1.3$ |
| $P_0 = P_1$ | $EoS1.1$ | $EoS1.1$ | $EoS1.1$ | $LE1.3$ |
| $P_2 < P_0 < P_1$ | $EoS1.2$ | $EoS1.2$ | - | - |
| $P_1 < P_0 < P_2$ | - | - | $EoS1.2$ | $LE1.3$ |
| $P_0 = P_2$ | $EoS1.3$ | $EoS1.2$ | $EoS1.2$ | $LE1.3$ |
| $0 < P_0 < P_2$ | $EoS1.4$ | $EoS1.2$ | $EoS1.2$ | $LE1.3$ |
| $P_0 = 0$ | $HE1.1$ | $HE1.2$ | $HE1.2$ | $HE1.3$ |
| $P_0 < 0$ | $LE2.3$ | $LE2.3$ | $LE2.3$ | $LE2.3$ |

The subcases in which the phase space has a different topology from the ones seen in the previous chapters are the following:

- *EoS*1.1: $\alpha < -1$, $P_0 = P_1$. By choosing $\alpha = -7/3$ and $\beta = 1$, we have that $P_0 = P_1 = 1$ and we obtain the following phase portrait:

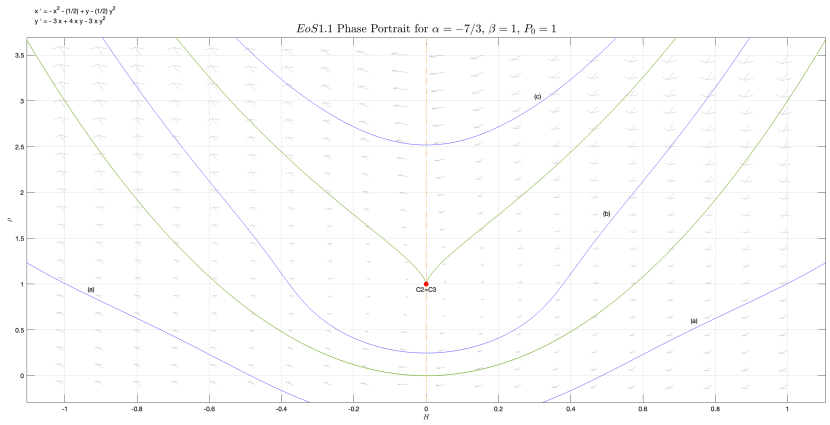


  Only one fixed point exists within this subset of conditions, it is given by the two generalized static Einstein universes C2 and C3, that here are coinciding. The fluid is standard, but not all models are acceptable. In fact, the open universes such as (a) are nonphysical as their evolution involves the $\rho < 0$ portion of the phase space. The lower green line represents the parabola given by the Friedmann equation for $K = 0$, that is all the flat models, which in this case is just one single solution. The flat model evolves as the closed universes of the (b)-type and (c)-type do, in a turn-around fashion: they leave a Type III singularity while expanding, the maximum $a$ and minimum $\rho$ are reached, then the contraction takes place and a Type III singularity is approached again in the future. The solutions that lie on the stable orbits represented by the upper green lines respectively leave/approach (left/right) a Type III singularity towards/from the static universe C2=C3. This subcase corresponds to the condition *G1.*

- *EoS*1.2: $\alpha < -1$, $P_2 < P_0 < P_1$. We set $\alpha = -2$ and $\beta = 1$, so that $1/4 < P_0 < 25/36$ and we choose $P_0 = 1/2$ for the following phase portrait:

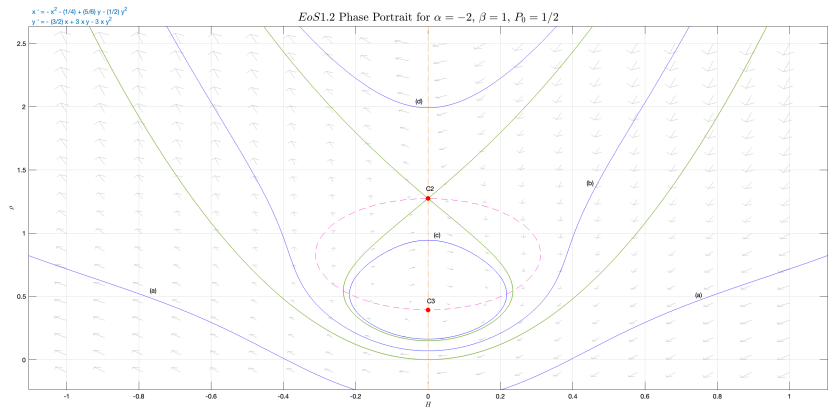


  The fluid behaves in a standard manner and the only difference from the previous subcase is that C2 and C3 divide into two distinct points, the first being a saddle and the latter a center. The new solutions that arise are those closed universes of the (c)-type which evolve in closed loops centered in C3, they alternate phases of expansion and contraction, reaching respectively a maximum $a$

(minimum $\rho$) and a minimum $a$ (maximum $\rho$). The green orbit that surrounds C2 expands and re-contracts from/to the generalized Einstein universe in C3. Once again, we are in the *G1* condition.

- *EoS*1.3: $\alpha < -1$, $P_0 = P_2$. We set $\alpha = -3$ and $\beta = 1$, so $P_0 = P_2 = 1$ and the following phase portrait is obtained:

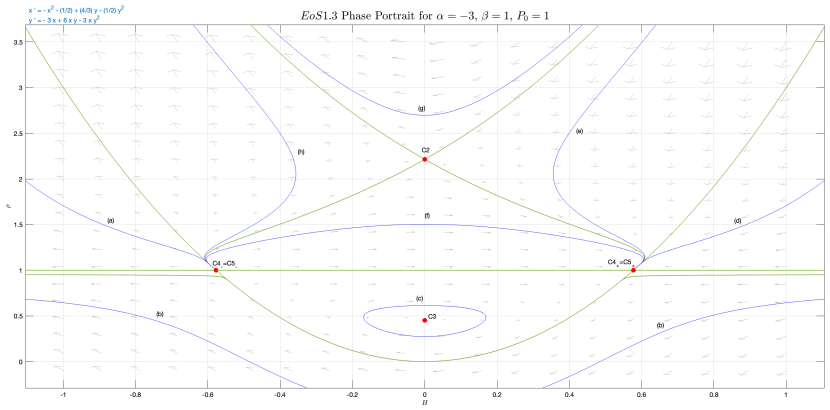


Here the behaviour is richer: with this choice of parameters the existence conditions for the de Sitter universes $C4_{\pm}$ and $C5_{\pm}$ are met. We are in the presence of four fixed points, since $C4_+$ and $C5_+$, $C4_-$ and $C5_-$ coincide. The phantom separatrix $\rho = \bar{\rho}_\Lambda$ - which connects the fixed de Sitter universes - appears, dividing the lower region (*H1*) from the upper one (*H2*), both with standard behaviour. (a) and (d) are open models and they reach/leave a Type III singularity from/to the contracting/expanding de Sitter fixed points. (b) is nonphysical, (c) evolves in the same way as it did in *EoS*1.2. (e) and (h) respectively leave/approach a Type III singularity to/from the expanding/contracting de Sitter fixed points, they are closed models. The (f)-type solutions also represent closed models which contract from $C4_-$ to a minimum $a$ (maximum $\rho$) and then expand to $C4_+$ in the future. The solutions in the region where (g) lies are, once again, standard closed turn-around models which leave and then reach again a Type III singularity. Flat solutions leaving the de Sitter fixed points in the region below the phantom separatrix do not terminate on the symmetrical fixed point, instead they are asymptotical to the separatrix, that is they continue contracting/expanding at an increasing rate towards a finite value of the energy density. On the other hand, the remaining non-fixed flat models, that is the ones in the $\rho > \bar{\rho}_\Lambda$ region, are asymptotical to a Type III singularity. Lastly, there two stable orbits (in green) that leave $C4_{\pm}$ towards the generalized Einstein point C2; from there, the other two solutions that approach/leave C2 do so leaving/approaching a Type III singularity.

- *EoS*1.4: $\alpha < -1$, $0 < P_0 < P_2$. We set $\alpha = -4$ and $\beta = 1$, so that $P_2 = 9/4$ and we choose $P_0 = 1$. The following phase portrait is obtained:

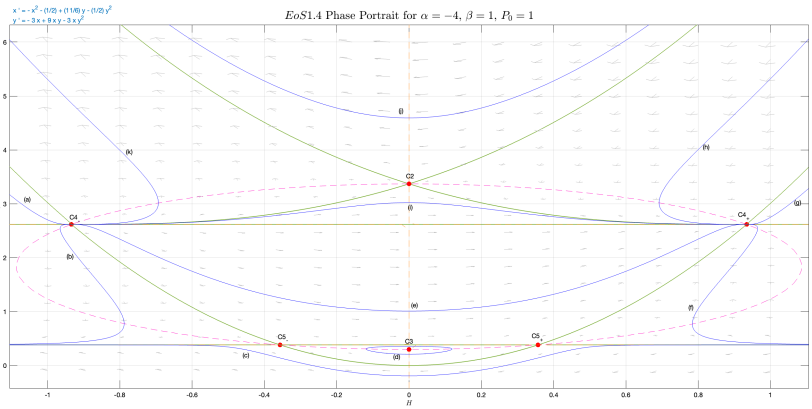


Here the generalized flat de Sitter points $C4_{\pm}$ and $C5_{\pm}$ split, generating an horizontal phantom separatrix which connects $C4_{-}$ and $C4_{+}$, as well as one that connects $C4_{-}$ and $C4_{+}$. The upper separatrix corresponds to $\rho = \rho_{\Lambda,1}$, the lower one to $\rho = \rho_{\Lambda,2}$, they divide the phase space into three regions. The lower and upper regions respectively satisfy the conditions *I1* and *I3*, whilst the middle region corresponds to *I2* and it portrays a phantom behaviour. The qualitative differences in respect to the subcase *EoS*1.3 are found in the *I2* region: open models such as (b) and (f) are asymptotical to the effective cosmological constants; (b) leaves $C4_{-}$ and tends to $\rho_{\Lambda,2}$ in the future, (f) leaves $\rho_{\Lambda,2}$ and towards $C4_{+}$. The non-fixed flat models in this region evolve by moving between $C4_{-}$ and $C5_{+}$ whilst contracting, or between $C5_{+}$ and $C4_{+}$ whilst expanding. The (e)-type solutions are the only closed models in this region and they move from $C4_{-}$ to $C4_{+}$, at first contracting to a minimum scale factor (and energy density), then re-expanding.

## 0.17 *EoS*2: $\beta < 0$

For the case $\beta < 0$ the qualitative similarities with the phase portraits present in the script are the following:

| | $\alpha < -1$ | $-1 \leq \alpha < -2/3$ | $-2/3 \leq \alpha < -1/3$ | $-1/3 \leq \alpha$ |
|---|---|---|---|---|
| $P_0 > 0$ | *LE*1.1 | *LE*1.1 | *LE*1.1 | *LE*1.1 |
| $P_0 = 0$ | *HE*2.1 | *HE*2.2 | *HE*2.2 | *HE*2.3 |
| $P_1 < P_0 < 0$ | *LE*2.1 | *EoS*2.3 | *EoS*2.3 | *EoS*2.1 |
| $P_0 = P_1$ | *LE*2.1 | *EoS*2.3 | *EoS*2.3 | *EoS*2.2 |
| $P_2 < P_0 < P_1$ | - | - | *EoS*2.3 | *EoS*2.3 |
| $P_1 < P_0 < P_2$ | *LE*2.1 | *EoS*2.3 | - | - |
| $P_0 = P_2$ | *LE*2.1 | *EoS*2.4 | *EoS*2.4 | *EoS*2.4 |
| $P_0 < P_2$ | *LE*2.1 | *LE*2.1 | *LE*2.1 | *LE*2.1 |

The subcases with a new kind of behaviour are:

- *EoS*2.1: $\alpha > -\frac{1}{3}$, $P_1 < P_0 < 0$. By setting $\alpha = 1$ and $\beta = -1$ we obtain $P_1 = -4/9$, finally setting $P_0 = -1/4$ we derive the following phase portrait:

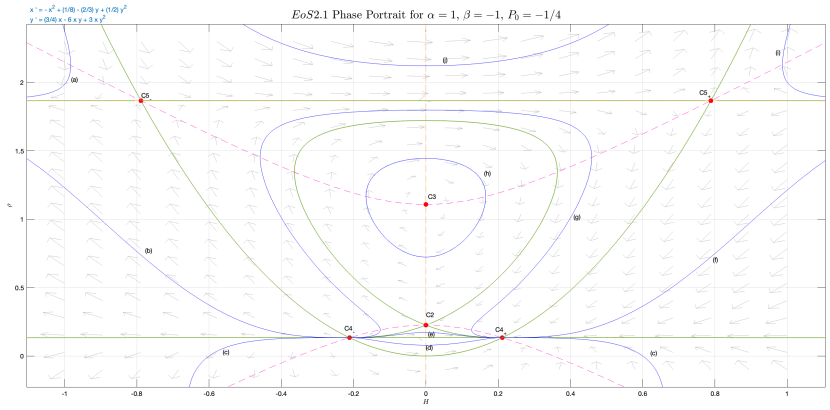


Here the upper horizontal separatrix is given by $\rho = \rho_{\Lambda,2}$ and it connects C5$_-$ to C5$_+$, the lower one by $\rho = \rho_{\Lambda,2}$ and it connects C4$_-$ to C4$_+$. These two separatrices divide the phase space into three regions, the fluid exhibits phantom behaviour in the upper (*I6*) and lower (*I4*) ones, whilst it behaves in a standard manner only in the central one (*I5*). (a) is open, it leaves a Type III singularity (asymptotically in respect to the flat model) in the past and continues contracting whilst approaching $\rho_{\Lambda,2}$ in the future, (i) is its symmetrical and it expands from $\rho_{\Lambda,2}$ to the Type III singularity. (b) and (f) are also open, they are asymptotical to $\rho_{\Lambda,2}$ and terminate, respectively in the past/future, in the flat contracting/expanding de Sitter fixed points. (c) is nonphysical, (d) is a closed phantom model in which the universe contracts from C4$_-$ to a minimum $a$ ($\rho$) and then expands to C4$_+$. (e) does the same as (d) but with a standard behaviour. The other closed orbits in the central region either loop around the generalized Einstein universe in C3, eventually the green stable orbits start/terminate from/in C2. (j) represents a turn-around model, and it undergoes a phantom bounce when the minimum for the scale factor is reached.

- *EoS*2.2: $\alpha > -\frac{1}{3}$, $P_0 = P_1$. We choose $\alpha = 1$ and $\beta = -1$, so $P_0 = P_1 = -4/9$. We obtain:

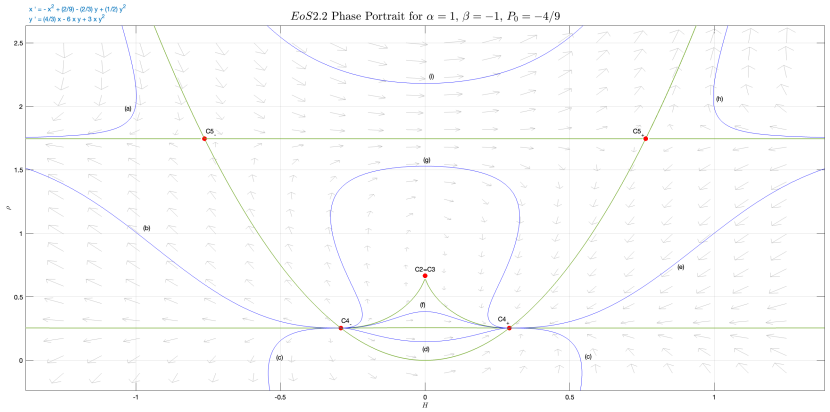


This subcase is similar to the previous one, the only difference being that the two generalized Einstein fixed points now coincide. This changes the possibilities for the closed models in the region, which evolve from C4$_-$ to C4$_+$ as (f) and (g) do, but there are no longer loop models where phases of contraction and expansion alternate in an infinite fashion. There exists also a closed solution that leaves C4$_-$ moving towards the static fixed point C2 while contracting, and one that leaves the latter to approach the expanding generalized de Sitter flat universe C4$_+$ in the future.

- *EoS*2.3: $\alpha > -\frac{1}{3}$, $P_2 < P_0 < P_1$. We choose $\alpha = 1$ and $\beta = -1$ once again, so that $-1 < P_0 < -4/9$ and we set $P_0 = -1/2$ to obtain the following phase portrait:

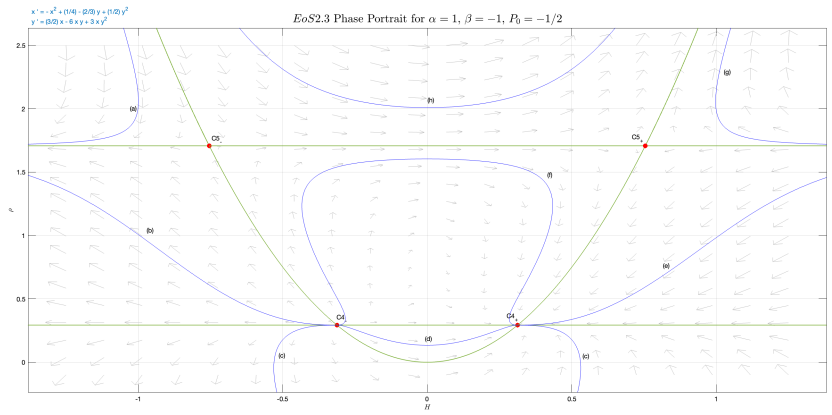


In this subcase the two generalized Einstein static universes do not exist, hence the closed models in the central region can only evolve by leaving C4$_-$ while contracting, reach a minimum $a$ (maximum $\rho$) and then re-expand into the generalized de Sitter flat universe in C4$_+$. The rest of the phase space remains the same as in the previous subcase.

- *EoS2.4*: $\alpha > -\frac{1}{3}$, $P_0 = P_2$. We set $\alpha = 1$, $\beta = -1$, thus $P_0 = P_2 = -1$, and we find the following phase portrait:

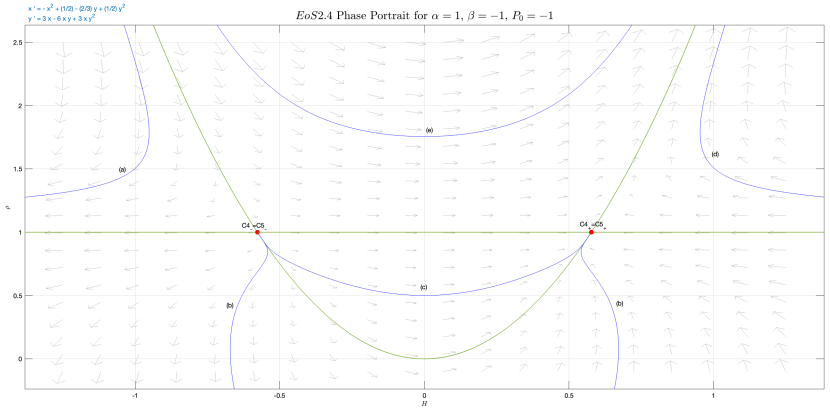


Here the two sets of generalized de Sitter fixed points coalesce, leaving only one horizontal separatrix of equation $\rho = \bar{\rho}_\Lambda$. We are in the $H$ set of conditions, specifically the upper region satisfies *H4* and the lower one *H3*: the behaviour is phantom in all of the phase space. The qualitative traits of the phase space are the same of *EoS2.2* and *EoS2.3*, except for the middle region that here is no longer present.

# Conclusions

In this script we started by presenting the essential results of GR necessary for model building in cosmology, we also adressed the current evidence of an accelerated expansion of our universe - and its link with the concept of dark energy - as well as the presence of extra mass (dark matter) that does not interact electromagnetically and of which we now have several proofs. The fluid equation has been presented and the importance of finding a barotropic EoS that describes the pressure contribute $P(\rho)$ has been stressed, for it is crucial in the description of the dynamics of the cosmos, the energy density content can then be derived via integration as a function of the scale factor $a(t)$. We pointed out that a specific EoS could account for the dark energy component and that it might also provide a description for dark matter, in the framework of UDM models. The scenario for which the cosmological fluid behaves as an effective cosmological constant term was adressed and the conditions that generate accelerated phases in the expansion of the universe were discussed. We saw that the fluid can behave in two different manners: a standard one, for which an increase in the scale factor causes a decrease in the energy density, and a phantom one, for which the dynamic is more counterintuitive as $a$ and $\rho$ increase/decrease accordingly. At this point we introduced the central object of our study: a specific form for the EoS. We chose the quadratic form (25), already studied by Ananda and Bruni in [1], which is significant for it is the Taylor expansion up to the second order of any $P(\rho)$ about 0, or after a regrouping of terms about the present energy density $\rho_0$ [10]. We divided the analysis into three regimes: the high energy regime; for which the constant pressure term can be neglected; the low energy regime, for which the quadratic term can be neglected; the complete EoS. The study was done via the theory of dynamical systems, a linear stability analysis was carried out for each fixed point and a phase portrait was shown for every subcase, that is for every subset of parameters that gave rise to different qualitative behaviours. The fixed points that we found were of three types: generalized Einstein universes, namely static solutions with a finite energy density; generalized de Sitter flat universes, with a constant (negative or positive) rate of expansion and a fixed energy density; a Minkowski universe, corresponding to a static, flat model with null energy density (the origin). We saw that the presence of such points and their dynamical nature depended on the specific subcase, in many cases small changes of one or more parameters gave rise to totally different topologies of the phase space. A main fact was that accelerated phases in the evolution of the universe were present in a lot of solutions and, for a substantial number of subcases, we found the presence of an effective cosmological constant (or two for the full EoS), with different orbits that were asymptotical to it in the past/future.

In the high energy regime we found phantom models (with all curvatures) that approach/leave an effective cosmological constant whilst leaving/approaching a null energy density (*C1*) - in this case $\rho_\Lambda$ is met at zero curvature - or whilst leaving/approaching a Type III singularity asymptotically to a flat universe (*B2*). Other phantom models (*A2*) can tend to a null energy density on one extreme and to a Type III singularity (asymptotically to $K = 0$) on the other, else they can undergo a phantom bounce, reaching both at early and late times the singularity. Standard models in the high energy regime can be asymptotical to an effective cosmological constant in the past/future and to a Type III singularity in the future/past, or undergo a turn-around by starting and ending in the singularity, there are also four orbits which start/end in a generalized Einstein universe (*B1*). Another possibility is for the standard fluid

to start/end with a null energy density while end/start in a Type III singularity (*A1*) or in an effective cosmological constant (*C2*). *A1* admits standard turn-around models to, on the other hand *C2* can also start/end (eventually also end/start) in a Minkowski universe, it presents the possibility for standard loop models (around a generalized Einstein universe) - namely universes that oscillate infinitely between maximum $a$ (minimum $\rho$) and minimum $a$ (maximum $\rho$) - as well.

In the low energy regime we found open and flat phantom solutions that are asymptotical to an effective cosmological constant in the past/future and to a Type I singularity (Big Rip) in the future/past, as well as closed turn-around models that start and end in a Type I singularity (*E1*), all these models have $K \to 0$ when they reach the singularity. Other phantom solutions in this regime can either tend to an effective cosmological constant in one extreme and to a null energy density (or again to the constant) on the other (*F2*), else they can be closed or flat models which start and end in a Big Rip (*D2*). The fluid can also exhibit standard behaviour and have the same dynamics, namely start and end in a Big Rip, possibly also loop around a closed generalized Einstein universe (*D1*). Other possibilities for standard solutions would be to approach both at early and at late times an effective cosmological constant (flat ones) or to loop (closed ones) around a generalized Einstein point (*F1*); else they can tend on one extreme to an effective cosmological constant and on the other one to a Big Bang/Big Crunch, or to a generalized Einstein universe, or once again to the effective cosmological constant (*E2*). In detail, in the subset *E2* we found models in which the standard fluid evolves as a closed universe from an early time Big Bang to approach, at late times, a flat generalized de Sitter point dominated by the effective cosmological constant.

When we adressed the full EoS we presented a list of subcases for which the topology of the phase space was qualitatively similar to the ones already reported, but we also found new types of possible behaviours for the solutions. For the phantom case we have flat and open solutions which can be asymptotical on both sides to two different effective cosmological constant terms, or closed ones asymptotical on both sides to one of the constants (*I2*). There are also phantom solutions which can start/end in a Type III singularity and end/start on an effective cosmological constant, or they can undergo a phantom bounce as turn-around models (*H4*, *I6*). Another possibility for the phantom fluids is to leave/approach a null energy density from/to a Type III singularity (*G2*). Lastly, some phantom solutions can evolve to/from a null energy density from/to an effective cosmological constant (*H3*, *I4*). For the standard case there is the possibility for a tendency, both in the past and in the future, to an effective cosmological constant (*I5*), the constant can also be approached in the past/future with a null energy density at late/early times (*H1*, *I1*). A Type III singularity is part of a subset of standard solutions and on the other side of the orbit the fluid can either approach a null energy density (*G1*) or an effective cosmological constant (*H2*, *I3*).

As we already said, we stress a focal point in the analysis was the discovery that in many subsets of parameters - in the various regimes - accelerated stages for the expansion (or contraction) of the cosmos were predicted. An effective cosmological constant term (or two) was present in diverse scenarios, with diverse solutions that displayed asymptotical tendencies towards such values. We found that generalized de Sitter fixed points were directly linked to the presence of an effective cosmological constant as they lied in the intersection between these constant values of the energy density and the parabola for flat models (the Friedmann equation for $K = 0$). Interestingly, such points were often attractors/repellers for a large enough class of solutions. This, all together, can provide for a possible description of dark energy in its effects. Our analysis, however, was limited to the study of the only quadratic EoS, hence it was aimed at showing the effects that this component has only when it is the dominant one in the cosmological fluid, that is when standard matter and radiation have not prevailing effects on the dynamics. Nonetheless, the significance of the study is given by the possibility that these components can - within certain subsets of conditions for the chosen EoS - coexist, allowing for dark energy to be the dominant in certain cosmic eras, such as the present one.

# Bibliography


[1] Ananda K.N., Bruni M., "Cosmological dynamics and dark energy with a nonlinear equation of state: A quadratic model", *Physical Review D 74, 023523*, 2006

[2] Bertacca D., Matarrese S., "Unified Dark Matter in Scalar Field Cosmologies", *Modern Physics Letters A*, Vol. 22, N0. 38 (2007) 2893-2907

[3] Fassò F., "Istituzioni di Fisica Matematica", *Cleup*, 2018

[4] Hobson M.P., Efstathiou G., Lasenby A.N., "General Relativity, An Introduction for Physicists", *Cambridge University Press*, 2006

[5] Liddle A., "An Introduction to Modern Cosmology, third edition", *Wiley*, 2015

[6] Misner C.W., Thorne K.S., Wheeler J.A., "Gravitation", *Princeton University Press*, 2017

[7] Tong D., "Cosmology", *https://www.damtp.cam.ac.uk/user/tong/teaching.html*, 2019

[8] Riess A. G. *et al.*, Astron. J. 116, 1009 (1998); Perlmutter S. *et al.*, Astrophys. J. 517, 565 (1999); Riess A.G. *et al.*, Astrophys. J. 607, 665 (2004)

[9] Weinberg S., Rev. Mod. Phys. 61, 1 (1989)

[10] Visser M., Classical quantum gravity 21, 2603 (2004)

[11] Caldwell R.R., Phys. Lett. B 545, 23 (2002)

[12] Carroll. S., "Spacetime and Geometry: Introduction to General Relativity", *Addison Wesley, Boston 2003*

[13] Visser M., Science 276, 88 (1997); Phys. Rev. D 56, 7578 (1997)

[14] Nojiri S., Odintsov S.D., Tsujikawa S., Phys. Rev. D 71, 063004 (2005)

[15] Stefancic H., Phys Rev. D 71, 084024 (2005); 71, 124036 (2005)

[16] Barrow J.D., Classical Quantum Gravity 21, 5619 (2004); 21, L79 (2004)

[17] Zendri J.P., "Introduction to General Relativity", personal notes from the lectures held at the University of Padua for the undergraduate course in Physics, 2022